AD-A147 888 STRUCTURAL RELAXATION AND ISOCONFIGURATIONAL FLOW OF A METALLIC GLASS NEA.. (U) HARVARD UNIV CAMBRIDGE MA DIV OF APPLIED SCIENCES S S TSAO ET AL. AUG 84 TR-25 1/1

UNCLASSIFIED N00014-77-C-0002 F/G 11/2 NL

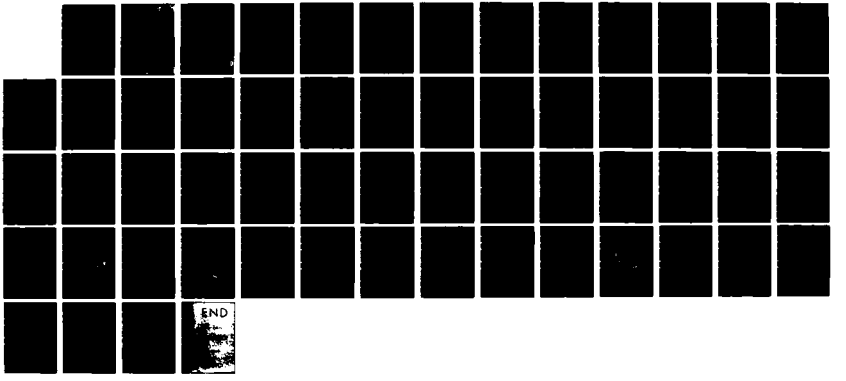

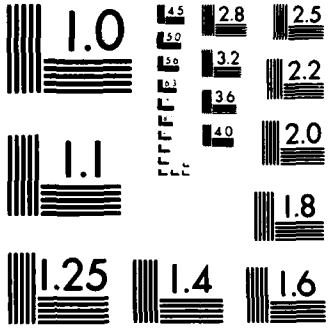

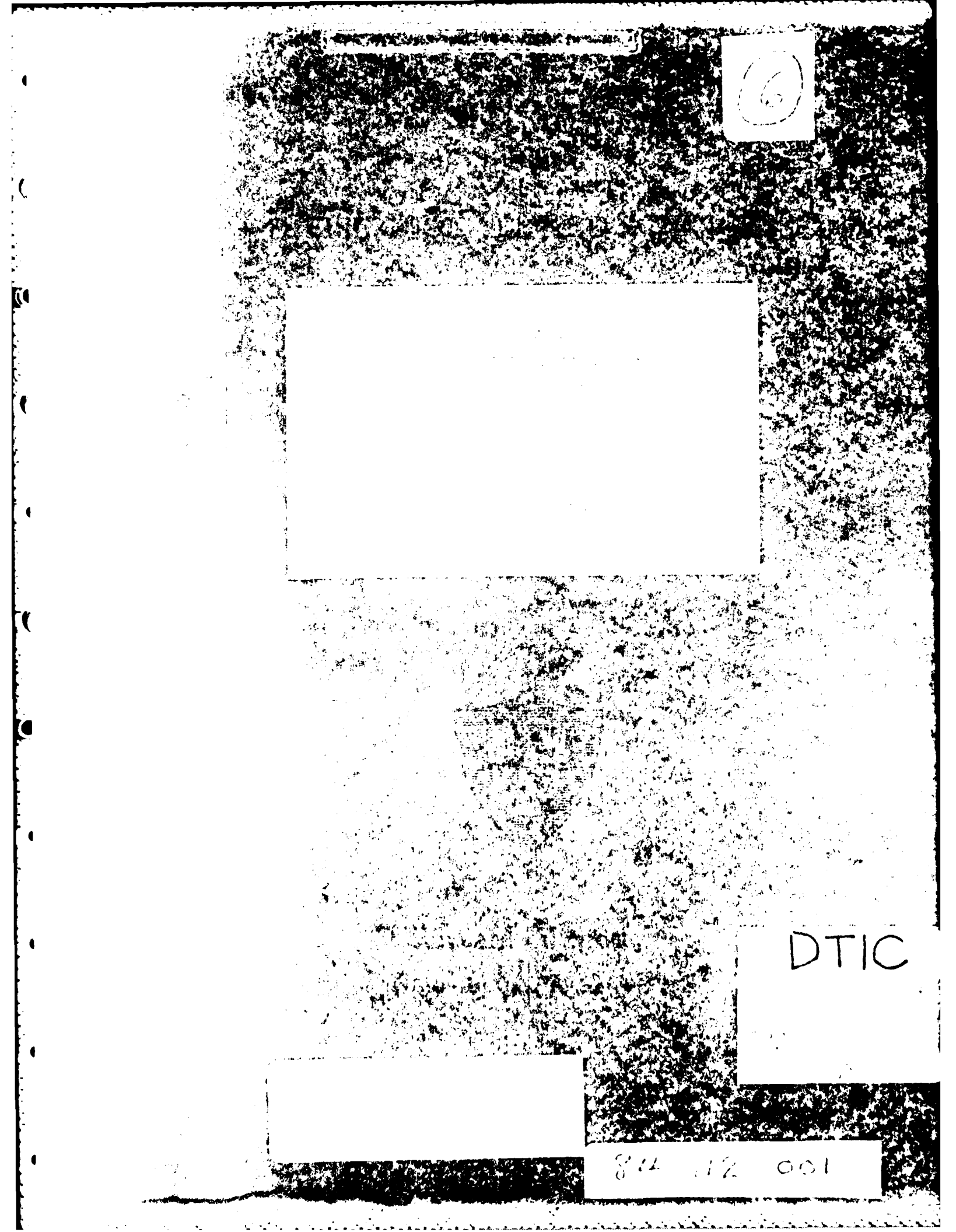
DTIC

Office of Naval Research

Contract Number N00014-77-C-0002

# STRUCTURAL RELAXATION AND ISOCONFIGURATIONAL FLOW OF A METALLIC GLASS NEAR EQUILIBRIUM

by

S.S. Tsao and F. Spaepen

Technical Report No. 25



August 1984

The research reported in this document was made possible through support extended the Division of Applied Sciences, Harvard University by the Office of Naval Research, under Contract N00014-77-C-0002.

Division of Applied Sciences

Harvard University · Cambridge, Massachusetts

| REPORT DOCUMENTATION PAGE | | READ INSTRUCTIONS BEFORE COMPLETING FORM |
|---|---|---|
| 1. REPORT NUMBER<br>Technical Report No. 25 | 2. GOVT ACCESSION NO.<br>A147 888 | 3. RECIPIENT'S CATALOG NUMBER |
| 4. TITLE (and Subtitle)<br>STRUCTURAL RELAXATION AND ISOCONFIGURATIONAL FLOW OF A METALLIC GLASS NEAR EQUILIBRIUM | | 5. TYPE OF REPORT & PERIOD COVERED<br>Interim Report<br>6. PERFORMING ORG. REPORT NUMBER |
| 7. AUTHOR(s)<br>S.S. Tsao and F. Spaepen | | 8. CONTRACT OR GRANT NUMBER(s)<br>N00014-77-C-0002 |
| 9. PERFORMING ORGANIZATION NAME AND ADDRESS<br>Division of Applied Sciences<br>Harvard University<br>Cambridge, Massachusetts 02138 | | 10. PROGRAM ELEMENT, PROJECT, TASK AREA & WORK UNIT NUMBERS |
| 11. CONTROLLING OFFICE NAME AND ADDRESS | | 12. REPORT DATE<br>August 1984<br>13. NUMBER OF PAGES |
| 14. MONITORING AGENCY NAME & ADDRESS(if different from Controlling Office) | | 15. SECURITY CLASS. (of this report)<br>Unclassified<br>15a. DECLASSIFICATION/DOWNGRADING SCHEDULE |

16. DISTRIBUTION STATEMENT (of this Report)

This document has been approved for public release and sale; its distribution is unlimited. Reproduction in whole or in part is permitted by the U.S. Government.

17. DISTRIBUTION STATEMENT (of the abstract entered in Block 20, if different from Report)

18. SUPPLEMENTARY NOTES

19. KEY WORDS (Continue on reverse side if necessary and identify by block number)

amorphous metals, metallic glasses, viscosity, creep, isoconfigurational flow, structural relaxation, bimolecular kinetics, annealing effects, glass transition temperature, Fulcher-Vogel equation

20. ABSTRACT (Continue on reverse side if necessary and identify by block number)

The non-linear viscosity change as a result of structural relaxation near equilibrium, at temperatures below and above the fictive temperature, has been measured for amorphous $Pd_{77.5}Cu_6Si_{16.5}$. The viscosity increase is best described by bimolecular annihilation kinetics of flow defects. The viscosity decrease is described equally well by either unimolecular or bimolecular creation kinetics of flow defects.

-- continued --

From the asymptotic values of the model fits to the data, the equilibrium viscosity was determined. Over the temperature range 608 to 630K, the temperature dependence of the equilibrium viscosity, $\eta_{eq}$, of $Pd_{77.5}Cu_6Si_{16.5}$ is well described by the Fulcher-Vogel equation.

The isoconfigurational viscosity of amorphous $Pd_{77.5}Cu_6Si_{16}$ in various states of structural relaxation was investigated over a wide temperature range. It was found to be thermal history dependent and non-Arrhenian. The lower the glass fictive temperature, and hence the more ordered the glass, the greater the departure from Arrhenian behavior. The non-Arrhenian behavior shows that the temperature dependence of the isoconfigurational viscosity cannot be ascribed entirely to the temperature dependence of the jump frequency of the flow defect. The observed crossover of isoconfigurational curves obtained from different structural states implies that the isoconfigurational viscosity cannot be a function of only a single structural parameter, such as the average free volume of the specimen.

TABLE OF CONTENTS

# EFFECTS OF ANNEALING ON THE ISOCONFIGURATIONAL FLOW OF A METALLIC GLASS

S. S. Tsao* and F. Spaepen

Division of Applied Sciences, Harvard University
29 Oxford Street, Cambridge, MA 02138, U.S.A.

## ABSTRACT

The isoconfigurational viscosity of amorphous $Pd_{77.5}Cu_6Si_{16}$ in various states of structural relaxation was investigated over a wide temperature range. It was found to be thermal history dependent and non-Arrhenian. The lower the glass fictive temperature, and hence the more ordered the glass, the greater the departure from Arrhenian behavior. The non-Arrhenian behavior shows that the temperature dependence of the isoconfigurational viscosity cannot be ascribed entirely to the temperature dependence of the jump frequency of the flow defect. The observed crossover of isoconfigurational curves obtained from different structural states implies that the isoconfigurational viscosity cannot be a function of only a single structural parameter, such as the average free volume of the specimen.

---

*Present address: Sandia National Laboratories, Albuquerque, NM 87115, U.S.A.

## 1. INTRODUCTION

For measurements of the temperature dependence of the viscosity, $\eta(T)$, of an amorphous metal in its (unstable) glassy state to be physically meaningful, they must be <u>isoconfigurational</u>.

For example, if the viscosity were simply measured at increasingly higher temperatures, as a result of structural relaxation, which causes continuous viscosity increase, the apparent activation energy could be too low, and physically meaningless.

In an ideal isoconfigurational flow experiment, the viscosity of the same structure (i.e., one in which the relative positions of the atoms remain, at least statistically, the same) is measured as a function of temperature. In the Newtonian regime, the viscosity can be written as [1]:

$$\eta = \frac{kT}{n_f k_f' (\gamma_o v_o)^2} \qquad (1)$$

($n_f$: concentration of atomic scale sites producing shear, or ''flow defects''; $k_f'$: stress unbiased jump frequency of a shear defect; $\gamma_o$: shear strain per jump of a defect; $v_o$: volume of a defect). The temperature dependence of $\eta$ is, in general, dominated by the product $n_f k_f'$. The atomistic interpretation of the results from an ideal isoconfigurational experiment is then straightforward: the number of defects remains constant; therefore the temperature dependence of the isoconfigurational viscosity $\eta_{iso}(T)$ reflects only changes in the jump frequency $k_f'$.

In practice, however, it is difficult to ascertain experimentally that these ideal isoconfigurational conditions are achieved. All ''isoconfigurational'' measurements are therefore only defined in an

operational sense; i.e., the effects of irreversible structural relaxation are eliminated, but nothing is a priori known about possible reversible changes in the atomic structure of the glass.

In one type of isoconfigurational experiment, the temperature of the system, initially held at equilibrium, is rapidly changed by a small amount, and the instantaneous viscosity change determined by extrapolation of the viscosity transient back to the time when the new temperature was reached [2]. This type of isoconfigurational experiment is suitable for easy glass formers, such as silicates and polymers.

For metallic glasses, this technique is less suitable, since the approach to (metastable) equilibrium is often accompanied by rapid crystallization. Isoconfigurational experiments on metallic glasses must therefore be performed mostly below the glass transition temperature, $T_g$. Although structural relaxation in these experiments leads to viscosity increases with time (at temperatures below the fictive temperature, $T_f$), and even linearly far from equilibrium, the relative rate of increase $d(\ln \eta)/dt$, decreases with time. By structurally relaxing the specimen for a sufficiently long time, one can measure the viscosity at a number of different temperatures, return to the original temperature and find that the viscosity has not changed measurably. Since a typical viscosity measurement requires a total strain of only $10^{-4}$, the total number of atomic jumps during the experiment (assuming $\gamma_o \simeq 1$) is only one in $10^4$. This explains why isoconfigurational measurements of this type are possible, since the effects of irreversible atomic jumps on the structure can be minimized. The basic feature of this type of isoconfigurational experiment is thus reproducibility of the measurements on temperature cycling.

Several investigators have performed the second type of experiment on

metallic glass specimens far from equilibrium and found an Arrhenian temperature dependence of $\eta_{iso}(T)$. Taub and Spaepen measured activation energies, $Q_{iso}$, of 192kJ/mole and 240kJ/mole in $Pd_{82}Si_{18}$ [3] and $Pd_{77.5}Cu_6Si_{16.5}$ [4], respectively. Mulder et al. measured $Q_{iso}$ of 250kJ/mole in $Ni_{36}Fe_{32}Cr_{14}P_{12}B_6$ [5] and $Fe_{40}Ni_{40}B_{20}$ [6].

As discussed in an earlier paper [7], the straightforward interpretation of $Q_{iso}$ as simply reflecting Arrhenian temperature dependence of the jump frequency $k_f'$ (i.e. $n_f$ constant) poses a problem. In that case, the isoconfigurational viscosity would also have an Arrhenian form:

$$\eta_{iso}(T) = \eta_o^{iso} \exp (Q_{iso}/kT) \qquad (2)$$

with $\eta_o^{iso} = kT/n_f\nu_D(\gamma_o v_o)^2$ only weakly temperature dependent; $\nu_D$: Debye frequency.

For the first (i.e., least relaxed) set of the Taub and Spaepen isoconfigurational data on $Pd_{82}Si_{18}$ [3], $\eta_o^{iso} = 1.5\times10^{-7}Nsm^{-2}$, which is about four orders of magnitude lower than the expected value of about $10^{-3}Nsm^{-2}$ (viscosity of a liquid at high temperatures), and furthermore, is more than two orders of magnitude lower than the absolute minimum value that can be obtained from equation (2) (using $n_f = 1/\Omega$, $\nu_D = 10^{12}sec^{-1}$, $\gamma_o v_o = 3.4\Omega$ [8]; $\Omega$: atomic volume).

In view of this large discrepancy in the value of the pre-exponential, it seemed that isoconfigurational flow could not be considered to be a singly activated Arrhenian process. To test this we performed isoconfigurational experiments over a wider temperature range and closer to $T_g$. In the experiments of Taub and Spaepen [3,4] and Mulder et al. [5,6], each apparently Arrhenian isoconfigurational data set only spanned 40K or less.

These investigators also found $Q_{iso}$ to be the same for a number of structural states, i.e. independent of thermal history. In this paper, we report results of experiments designed to investigate the isoconfigurational behavior over a wide temperature range, particularly at temperatures close to $T_g$, and to determine whether $Q_{iso}$ remains independent of thermal history if the system is subjected to more markedly different annealing treatments.

## 2. EXPERIMENTAL PROCEDURE

Viscosity measurements were made using a tensile creep apparatus [9], modified as described previously [10]. The specimens were $Pd_{77.5}Cu_6Si_{16.5}$ disk-quenched ribbons and wires. The specimens were under load during the preanneals necessary to stabilize the amorphous structure prior to isoconfigurational testing. Stresses were kept low, from 21-144MPa to ensure Newtonian viscous flow. Due to the strong temperature dependence of the strain rate, test times varied from a few minutes at high temperatures to a few days at low temperatures. In early experiments, the stress was increased or decreased during the temperature cycling, depending on the direction of the temperature change, in order to extend the viscosity range of measurements within one isoconfigurational set.

In the last sets of experiments, $\eta_{iso}(T)$ was better characterized and wide-ranging isoconfigurational data sets (over 90K, and three orders of magnitude in $\eta_{iso}(T)$) were measured without any load changes. It is desirable to maintain the same load during temperature cycling since a load change induces anelastic strains that must be taken into account. For example, from loading-unloading experiments, we found that the anelastic strain contributes measurably to flow for about a day at 527K, and for about 6 minutes at 615K.

Thus longer test times are required for measurements after a load change, in order to allow for anelastic transient decay. Shorter test times are desirable to avoid structural relaxation.

## 3. RESULTS

Figure 1 summarizes the results on a $Pd_{77.5}Cu_6Si_{16.5}$ ribbon first annealed at 529K for 457 hours. Point 1 shows the final viscosity. The numbers indicate the order of the tests. After the measurement at point 4 with a test time of 24 hours, the shear stress was decreased from 144MPa to 96MPa and the sample held at the same low temperature of 501K for an additional 97 hours to allow for anelastic transient decay. Point 5 and, to a lesser degree point 6, are too high due to remaining transients from the load decrement at a temperature (501K) lower than the stabilization temperature (test 1, 529K).

Complete transient decay has likely occurred prior to the measurement at point 7. Points 1-20 trace out a first isoconfigurational curve, as demonstrated by cycling the temperature and reproducing the viscosity values. After the viscosity measurement at point 20, the specimen was allowed to relax at 588K for 40 hours. Point 21 shows the final viscosity. A second isoconfigurational curve (points 21-30) was then determined.

The results on a wire specimen, preannealed under load for 73 hours at 593K, are summarized in Fig. 2. Point 4 is too low due to transients after increasing the shear stress from 22MPa to 67MPa.

Figure 3 shows the results on a ribbon specimen first annealed at 593K for 4 hours. Point 1 is the viscosity at the end of the preanneal. Points 1-4 determine a first isoconfigurational set A, points 7-17 belong to a second

set B. The viscosity value shown at point 17 was measured at the start of a 19-hour anneal at 593K. Point 18 shows the final value. Points 18-30 trace out a third isoconfigurational curve C. The value shown at point 30 was measured at the start of a 24-minute anneal at 615K. Since this value is greater than the equilibrium viscosity, $\eta_{eq}$, at this temperature [10], the viscosity decreased with time to that shown at point 31. A fourth isoconfigurational set D (points 31-40) was then determined. The same specimen was then once again annealed at 593K for 24 hours. Points 42 and 43 show the viscosity values at the start and end of the anneal, respectively. A fifth isoconfigurational set E (points 43-52) was determined before the specimen was cooled to room temperature. The shear stress on the specimen was kept the same, at 53MPa, during the entire experiment. The viscosity change as a result of structural relaxation during the course of a viscosity measurement can be calculated from $\eta_{iso}$ and the relaxation rate, $\dot{\eta}$, determined from isothermal annealing experiments [10]. For example, during the 30 minutes test time to measure point 27, the viscosity is calculated to have changed by 0.2%. Optical microscopy of the tested specimen revealed <10 vol.% crystallinity, originating from the specimen surface. This amount of crystallinity is known to increase the viscosity gradually by at most ~25% [10] and to have very little effect on the magnitude of $Q_{iso}$.

## 4. DISCUSSION

Three basic observations can be made about the isoconfigurational data shown in Figs. 1-3: (i) the temperature dependence of isoconfigurational flow is inherently non-Arrhenian, (ii) $Q_{iso}(T)$ is dependent on the thermal history, and (iii) the isoconfigurational viscosity curves exhibit so-called crossover

behavior. The implications of these observations are discussed below.

The experimental isoconfigurational data for $\eta(T)$ are non-Arrhenian and therefore cannot be interpreted simply in terms of the temperature dependence of the jump frequency $k_f'$ (see equation (1)). The temperature dependence of the equilibrium viscosity, $\eta_{eq}(T)$, can be described well by the temperature dependence of $n_f(T)$ only [10,11]; thus the temperature dependence of $k_f'$ is probably quite weak. The isoconfigurational activation energy must therefore be accounted for by changes in $n_f$ and hence by some structural changes between each of the tests of an isoconfigurational set. Since the viscosity values can be reproduced upon temperature cycling, these structural changes must also be reversible.

The precise microscopic picture which leads to reversible changes in $n_f$ is still unclear. It appears, however, that some redistribution of the free volume change, resulting from the thermal expansion accompanying a test temperature change, must occur [7]. Microscopically, the structural changes could be described as fast, slight adjustments in the atom positions, without changes in nearest neighbors or chemical order.

The isoconfigurational data, particularly those shown in Fig. 3, clearly illustrate the thermal history dependence of $Q_{iso}(T)$. At testing temperatures far from $T_g$ ($T \leq 560K$), $Q_{iso}$ was lower if the fictive temperature of the specimen was lower, i.e. if the specimen was more ordered. For example, around 535K the magnitude of $Q_{iso}$ ranged between 0.4 and 2.0eV, depending on the state of annealing. For example, after annealing the same specimen above its fictive temperature (after set C in Fig. 3), thereby creating more disorder, the isoconfigurational curve D was obtained which exhibited a higher $Q_{iso}(T)$. Above 580K, $Q_{iso}$ remained nearly constant at $3.6 \pm .3$eV, regardless of thermal treatment. A temperature dependent $Q_{iso}$ has also been found in

amorphous $Pd_{82}Si_{18}$ [7].

The history independent Arrhenian behavior observed by other investigators [3,4,5,6] is reconciled with the results reported here as follows. The fictive temperatures of the specimens in the earlier tests were likely still quite high, since the preannealing treatments were performed at temperatures well below $T_g$. For example, Taub and Spaepen [4] preannealed their $Pd_{77.5}Cu_6Si_{16.5}$ specimen at temperatures between 500 and 552K for varying lengths of time, totalling about 24 days. Therefore, their data are expected to exhibit only a slight deviation from apparent Arrhenian behavior which is not likely to be noticed over their temperature span of 40K or less. Note that their data (shown as the dashed curve from 520 to 550K in Fig. 3) have a temperature dependence similar to those shown as curve B in Fig. 3, which were obtained from a specimen preannealed for a much shorter time, but at higher temperatures.

In the free volume model [12], $\eta_{eq}(T)$ is determined by the average free volume, $v_f$. Crossover of isoconfigurational curves obtained from the same specimen after various degrees of annealing treatments, for example as in the data shown in Figs. 1 or 3, implies that the same number of flow defects can be present in specimens of different average free volumes. Therefore, $\eta_{iso}(T)$ cannot be a function of only a single structural parameter, such as $v_f$, but that a second parameter such as the shape of the free volume (nonequilibrium) distribution curve must be taken into account.

## 5. CONCLUSIONS

The experimental results summarized in this paper show that isoconfigurational flow is inherently non-Arrhenian. Hence, the apparent

activation energy $Q_{iso}(T)$ cannot simply be ascribed to the temperature dependence of the jump frequency $k_f'$ and must be accounted for by changes in $n_f$ between each of the tests in an isoconfigurational set. Since $\eta_{iso}(T)$ is reproducible upon temperature cycling, the changes in $n_f$ must also be reversible. $Q_{iso}(T)$ is thermal history dependent. The value of $Q_{iso}(T)$ at $T \geq 580K$ was found to remain nearly the same ($3.6 \pm .3eV$) regardless of annealing treatment, whereas $Q_{iso}(T)$ at $T \leq 560K$ decreased with increasing degree of order in the specimen.

Crossover of isoconfigurational curves obtained from the same specimen at various stages of annealing imply that $\eta_{iso}(T)$ cannot be a function of only a single structural parameter.

ACKNOWLEDGMENTS

This work has been supported by the Office of Naval Research, Contract N00014-77-C-0002.

## FIGURE CAPTIONS

Figure 1. Isoconfigurational viscosity measurements on a $Pd_{77.5}Cu_6Si_{16.5}$ ribbon preannealed under load at 529K for 457 hours prior to the measurement at point 1. The numbers indicate the order of the tests. The light solid line is the equilibrium viscosity curve [10].

Figure 2. Isoconfigurational viscosity measurements on a $Pd_{77.5}Cu_6Si_{16.5}$ wire preannealed under load at 593K for 73 hours prior to the measurement at point 1.

Figure 3. Isoconfigurational viscosity measurements on a $Pd_{77.5}Cu_6Si_{16.5}$ ribbon preannealed under load at 593K for 4 hours prior to the measurement at point 1. The dashed line represents earlier measurements by Taub and Spaepen [4]. The light solid line is the equilibrium viscosity curve [10].

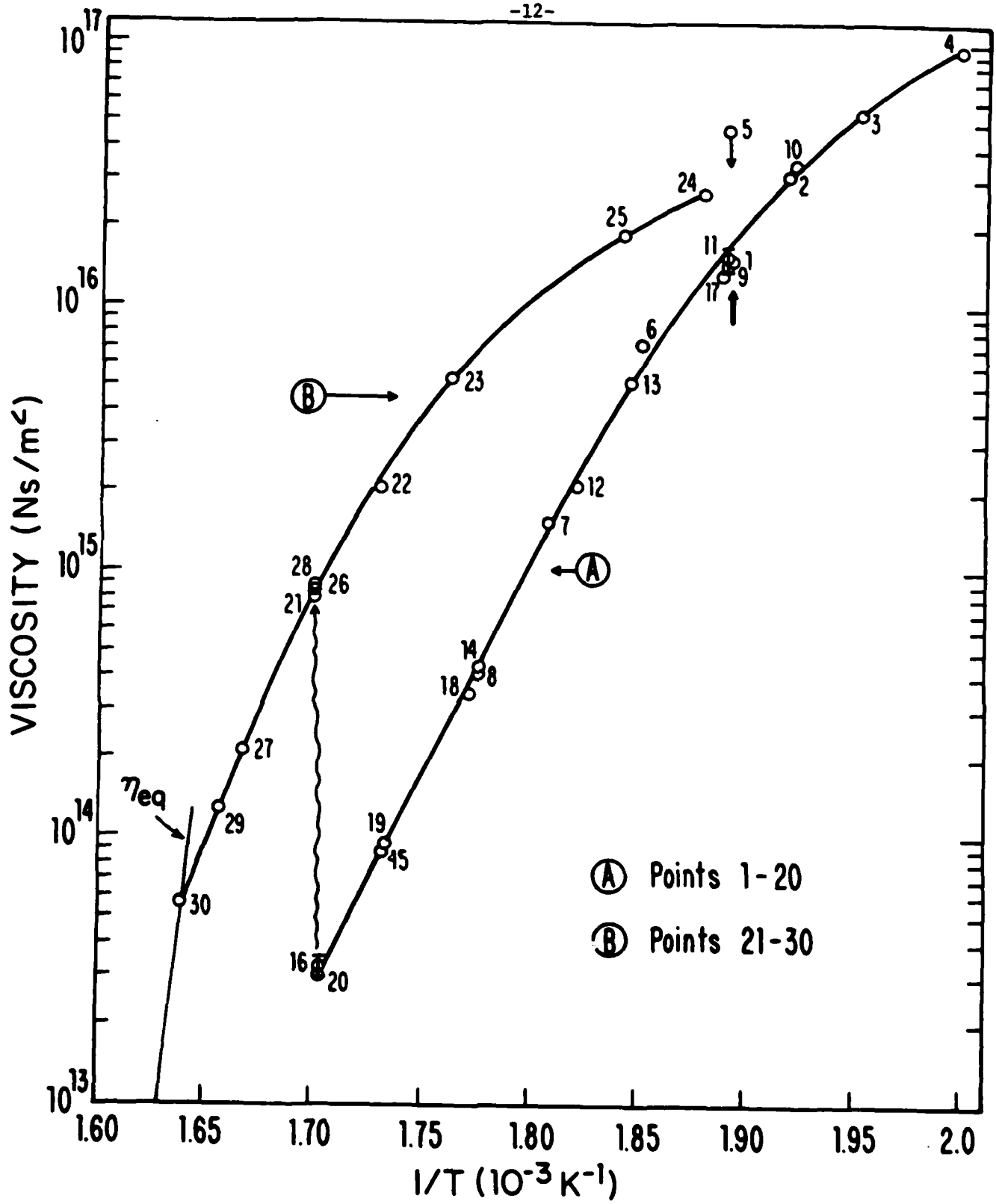


Figure 1

Isoconfigurational viscosity measurements on a $Pd_{77.5}Cu_6Si_{16.5}$ ribbon preannealed under load at 529K for 457 hours prior to the measurement at point 1. The numbers indicate the order of the tests. The light solid line is the equilibrium viscosity curve [10].

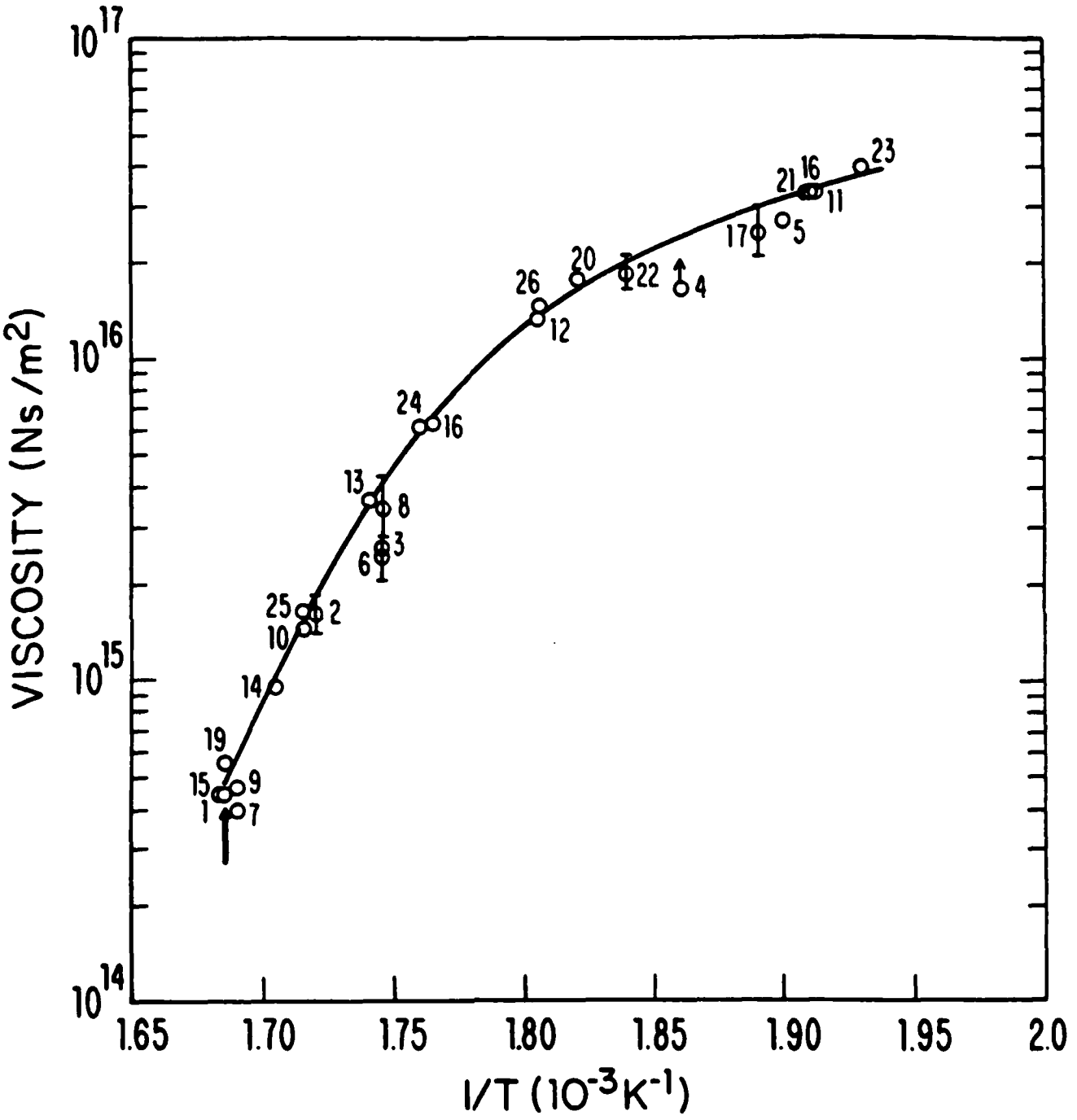


Figure 2

Isoconfigurational viscosity measurements on a $Pd_{77.5}Cu_6Si_{16.5}$ wire preannealed under load at 593K for 73 hours prior to the measurement at point 1.

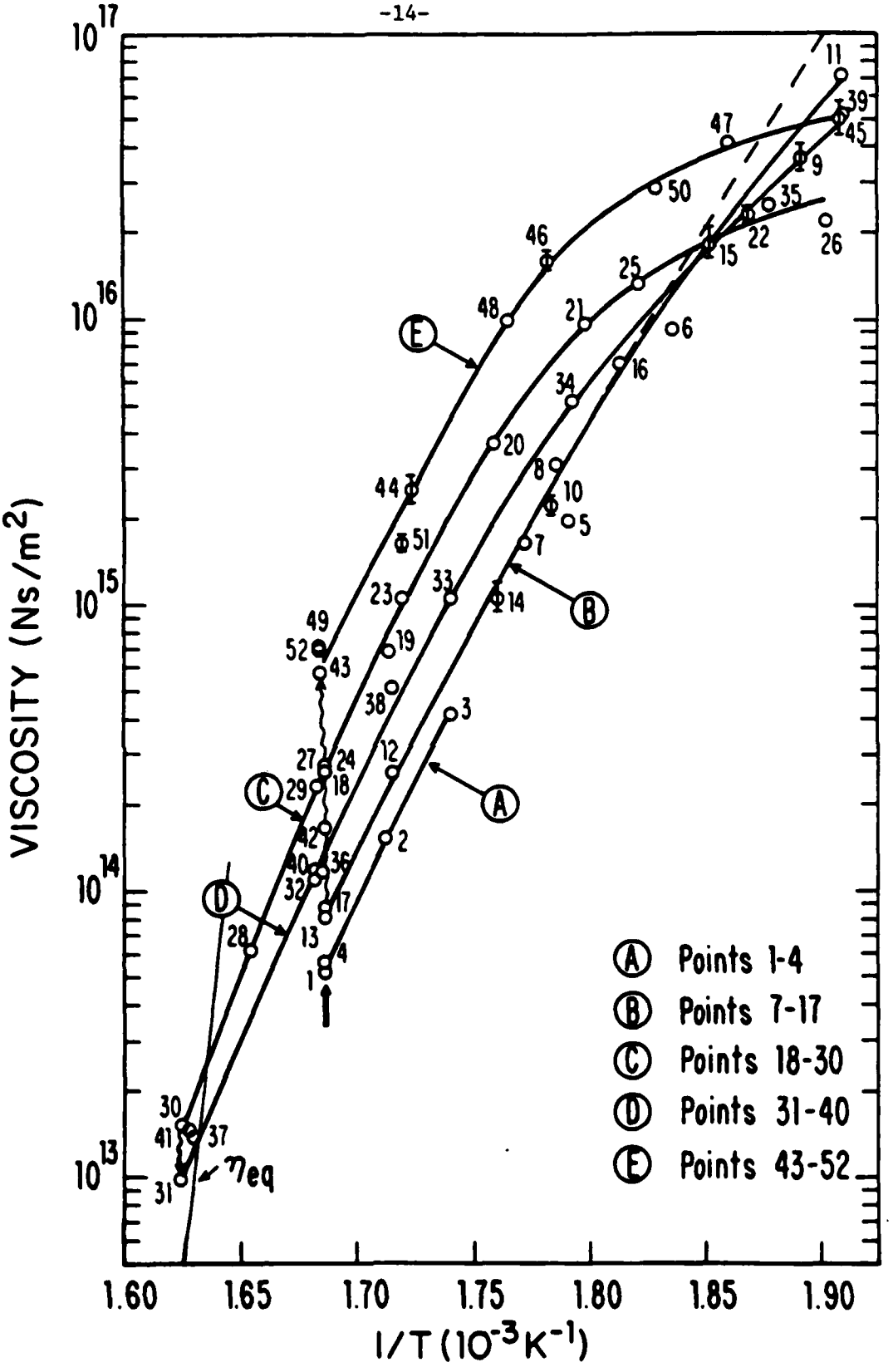


Figure 3

Isoconfigurational viscosity measurements on a $Pd_{77.5}Cu_6Si_{16.5}$ ribbon preannealed under load at 593K for 4 hours prior to the measurement at point 1. The dashed line represents earlier measurements by Taub and Spaepen [4]. The light solid line is the equilibrium viscosity curve [10].

## REFERENCES


1. F. Spaepen, ''Physics of Defects'', in Les Houches Lectures XXV, ed. by J.P. Poirier and M. Kleman, North Holland, 1981.
2. R.B. Stephens, J. Appl. Phys., 49, 5855 (1978).
3. A.I. Taub and F. Spaepen, Acta Met. 28, 1781 (1980).
4. A.I. Taub and F. Spaepen, Scripta Met. 14, 1197 (1980).
5. A.L. Mulder, J.W. Drijver and S. Radelaar, J. de Phys. 41, C-8 (1980).
6. A.L. Mulder, R.J.A. Derksen, J.W. Drijver and S. Radelaar, P. 1345, in Proc. 4th Int. Conf. on Rapidly Quenched Metals (Sendai, 1981).
7. S.S. Tsao and F. Spaepen, in Proc. 4th Int. Conf. on Rapidly Quenched Metals (Sendai, 1981).
8. A.I. Taub, Acta Met. 28, 633 (1980).
9. A.I. Taub and F. Spaepen, Scripta Met. 13, 195 (1979).
10. S.S. Tsao and F. Spaepen, to be published.
11. H.S. Chen and D. Turnbull, J. Chem. Phys. 48, 2560 (1968).
12. M. Cohen and D. Turnbull, J. Chem. Phys. 31, 1164 (1959).

# STRUCTURAL RELAXATION OF A METALLIC GLASS NEAR EQUILIBRIUM

S.S. Tsao* and F. Spaepen

Division of Applied Sciences, Harvard University
29 Oxford Street, Cambridge, MA 02138, U.S.A.

## ABSTRACT

The non-linear viscosity change as a result of structural relaxation near equilibrium, at temperatures below and above the fictive temperature, has been measured for amorphous $Pd_{77.5}Cu_6Si_{16.5}$. The viscosity increase is best described by bimolecular annihilation kinetics of flow defects. The viscosity decrease is described equally well by either unimolecular or bimolecular creation kinetics of flow defects.

From the asymptotic values of the model fits to the data, the equilibrium viscosity was determined. Over the temperature range 608 to 630K, the temperature dependence of the equilibrium viscosity, $\eta_{eq}$, of $Pd_{77.5}Cu_6Si_{16.5}$ is well described by the Fulcher-Vogel equation.

---

*Present address: Sandia National Laboratories, Albuquerque, NM 87115, U.S.A.

## 1. INTRODUCTION

An as-prepared metallic glass is thermodynamically unstable: it can lower its free energy continuously by a series of structural changes toward the metastable equilibrium configuration. This phenomenon is called ''structural relaxation'', and is manifested by continuous changes in all physical properties. The largest changes are observed for the atomic transport coefficients such as the shear viscosity, $\eta$, and atomic diffusivity, D. Most measurements of the effect of relaxation on the viscosity have so far been made at temperatures well below the glass transition temperature to avoid crystallization. At these low temperatures, where the glass is necessarily far from equilibrium, the viscosity has been observed to increase linearly with time, i.e. $\dot{\eta}$ is a constant [1,2,3,4]. This is illustrated schematically by line AB in Fig. 1. However, as demonstrated by Chen and Turnbull for a AuGeSi metallic glass [5], when the structure of the glass approaches its equilibrium configuration (line DE on Fig. 1), the rate of the viscosity rise decreases, since the viscosity must arrive at a unique, finite, equilibrium value, $\eta_{eq}(T)$ (point E on Fig. 1). Although measurements of $\eta_{eq}$ itself have been reported for metallic glasses (for example on AuGeSi), prior to our work described, no quantitative experimental study has been made of the viscosity relaxation kinetics of the <u>approach</u> to $\eta_{eq}$ near equilibrium.

In this paper, we present new measurements of viscosity relaxation near equilibrium, and compare the results with the predictions of a number of phenomenological models. Measurements near equilibrium were made possible by using a crystallization-resistant amorphous alloy, $Pd_{77.5}Cu_6Si_{16.5}$. Non-linear viscosity relaxation (i.e., $\dot{\eta}$ not constant in time) from <u>both</u> below and above $\eta_{eq}$ was observed (respectively DE and CE in Fig. 1). The phenomenological description of the relaxation near equilibrium is shown to be

in accord with the linear viscosity increase observed far from equilibrium.

The functional form of $\eta_{eq}(T)$ is of fundamental interest as a test of theoretical models of liquids and glasses. Because many metallic glasses tend to crystallize before reaching their fully relaxed state, the equilibrium viscosity, $\eta_{eq}(T)$, is often very difficult to measure directly. We will demonstrate how values of $\eta_{eq}(T)$ can be extracted from the extrapolated asymptotic behavior of the relaxation data. Coincidence of the asymptotic values for increasing and decreasing viscosities (DE and CE on Fig. 1) provides an experimental check on the accuracy of the determination of $\eta_{eq}$.

A preliminary report on the early stages of this work has been published [6]. In the present paper, the complete data and the full quantitative analysis of both the relaxation kinetics and equilibrium viscosity are presented.

## 2. EXPERIMENTS

The material used in these experiments was glassy $Pd_{77.5}Cu_6Si_{16.5}$ produced by disk quenching as a long, continuous ribbon, 13μm thick and 0.22mm wide, from which all specimens were cut. The amorphous nature of the specimens was verified by x-ray diffraction and differential scanning calorimetry. The glass transition and kinetic crystallization temperature were measured to be 636 and 674K, respectively at 20K/min.

The viscosity measurements were made using the tensile creep apparatus described previously [7]. Due to the high test temperatures, the tests were performed in air; no silicone oil was used. Nevertheless, the spatial temperature profile of the furnace remained very satisfactory: the temperature variation within the defined gage length of 3.1cm was only ±1/4K,

and, although the spatial temperature profile was not an ideal step function, the strain contribution from the specimen length outside the gage length was negligible, (less than 1% of the total strain), due to the strong temperature dependence of the strain rate. The warm-up time, from the holding temperature of 314K to the testing temperature, varied from 5 to 13 minutes, depending on the testing temperature and/or the controller settings. The temperature was maintained to $\pm 1/4$K during the anneals, which lasted from a few minutes to about a day. The furnace temperature was calibrated with the melting point of pure lead.

The high temperature runs typically produced total creep strains of 3-5%. The corresponding stress increase due to the cross-sectional area decrease was partially offset by geometrical changes in the creep apparatus. The error introduced by the assumption of constant stress is therefore quite small. The equivalent shear stress ranged from 7 to 35 MPa. Our experience showed that this stress range was still well within the Newtonian viscous regime.

Loading/unloading experiments were performed to ascertain that the observed viscosity behavior during the isothermal anneal is not affected by changes in the stress-strain rate sensitivity, $d\ln\dot{\gamma}/d\ln\tau$, the stress dependence of $\eta$ or anelastic transient decay.

The effects of stress changes on the viscosity of a specimen at 621K is shown in Fig. 2. Note that: (1) at this temperature the anelastic strain completely decays in a few minutes, (2) at these levels of stress and stress changes, the total anelastic strain is very small compared to the plastic strain, and (3) the relaxation kinetics are stress independent over the range of the test; save for short-lived deviations due to the presence of the transient after a load change, a smooth curve can be traced along the curves for $\eta$ at different stress levels.

The incremental anelastic strain $\Delta\gamma_A$ is determined by extrapolation of the steady-state strain back to the time when the stress change, $\Delta\tau$ was made. An anelastic compliance, $\Delta\gamma_A/\Delta\tau = 8.7 \pm 2.7 \times 10^{-11} m^2/N$ is obtained from the results in Fig. 2, in good agreement with Chen and Goldstein's measurements for the same alloy [8]. Results of tests at other temperatures are summarized in Table 1.

The ''noise'' on the viscosity curve of Fig. 2 is a result of the differentiation procedure used to determine the slope of the elongation curve. The continuous decrease of this slope leads to the increase in the signal-to-noise ratio with time, seen on Fig. 2 which is an experimental artifact without physical significance.

## 3. KINETICS OF VISCOSITY RELAXATION

### 3.1 Defect Relaxation Models

In the Newtonian regime, the viscosity can be written as [9]:

$$\eta = \frac{kT}{n_f k_f' (\gamma_o v_o)^2} \qquad (1)$$

($n_f$: concentration of microscopic sites producing shear, or ''flow defects''; $k_f'$: stress unbiased jump frequency of a shear defect; $\gamma_o$: shear strain per jump of a defect: $v_o$: volume of a defect). Theories, such as the free volume or configurational entropy models, can account for $\eta_{eq}(T)$ over a very large viscosity range entirely by a change in the equilibrium flow defect concentration $n_f(T)$. It is therefore reasonable to describe the nonequilibrium viscosity changes associated with structural relaxation by the

annihilation (or creation) of excess (or deficit) flow defects. Annihilation of flow defects can be thought to occur at special sites called relaxation defects. The rate of disappearance of flow defects, $n_f$, is then proportional to the product of the concentration of flow and relaxation defects, $n_f n_r$. However, since the system in equilibrium has a finite viscosity, $\eta_{eq}$, a number of defects, $n_{f,eq}$, must remain after an infinite annealing time. Kinetic laws in which $\dot{n}_f$ becomes zero when equilibrium is reached ($n_f = n_{f,eq}$) can be formulated, such as first- and second-order rate equations in the excess number of defects ($n_f - n_{f,eq}$). Respectively, for the unimolecular model:

$$\frac{d(n_f - n_{f,eq})}{dt} = - k_1(n_f - n_{f,eq}) \tag{2}$$

and for the bimolecular model:

$$\frac{d(n_f - n_{f,eq})}{dt} = - k_2(n_f - n_{f,eq})^2 \tag{3}$$

For the decreasing viscosity data, $k_2$ is negative. Equation (2) describes an annihilation mechanism where $n_r$ is constant whereas equation (3) describes an annihilation mechanism where $n_r \propto (n_f - n_{f,eq})$. If $n_r \propto n_f$, a third annihilation equation is:

$$\frac{d(n_f - n_{f,eq})}{dt} = - k_3 n_f(n_f - n_{f,eq}) \tag{4}$$

Integrating equations (2), (3) and (4) gives for the viscosity, respectively:

$$\frac{1}{\eta(t)} = \frac{1}{\eta_{eq}} + \left[\frac{1}{\eta_o} - \frac{1}{\eta_{eq}}\right] \exp(-k_1 t) \tag{5}$$

$$\frac{\eta(t)-\eta_o}{\eta_{eq}-\eta(t)} = \left[\frac{\eta_{eq}-\eta_o}{\eta_{eq}\ 2}\right] k_2 t \qquad (6)$$

$$\eta = \eta_{eq} - (\eta_{eq} - \eta_o)\exp(-k_3 t) \qquad (7)$$

Note that when $\eta_{eq} \gg \eta(t)$, as in low temperature relaxation experiments, or when $k_{1,3}t$ is small enough to allow first-order expansion of the exponential, all the above equations predict a linear viscosity increase with time.

The data exhibiting non-linear viscosity relaxation were fit mostly to the unimolecular and bimolecular equations (eqs. (5) and (6)) for two reasons. First, the bimolecular and unimolecular models have been shown to describe the viscosity increase and decrease, respectively, in silicate glasses [10,11]. The physical basis for this is discussed further in Section 5. Second, for several sets of increasing viscosity data fit to all three annihilation equations, the quality of the fit to eq. (7) obtained was intermediate between that of the other two equations. Therefore, fitting all the data sets to the third equation judged unlikely to give significant new information.

### 3.2 Results and Data Analysis

Since a quantitative comparison of the unimolecular and bimolecular fits is difficult with the noisy differentiated experimental viscosity curve, the fits were performed on the original elongation data. Equations (5) and (6) were therefore integrated to give expressions for the elongation change with time, respectively:

$$l(t) = l_o + K\left[\frac{t}{\eta_{eq}} + \frac{(\eta_{eq}-\eta_o)}{\eta_{eq}\eta_o k_1}(1-\exp(-k_1 t))\right] \qquad (8)$$

$$l(t) = l_o + K\left[\frac{(\eta_{eq}-\eta_o)}{\eta_{eq}^2 b}\ln\frac{\eta_o+\eta_{eq}bt}{\eta_o} + \frac{t}{\eta_{eq}}\right] \qquad (9)$$

K is the product of the shear stress and specimen gage length; b is equal to $(\eta_{eq}-\eta_o)k_2/\eta_{eq}^2$. Three free parameters, $\eta_{eq}$, $k_1$ or $k_2$ and the initial viscosity, $\eta_o$, together with the fixed experimental values for $l_o$ and K were used in fitting the data. A non-linear, multi-parameter fitting algorithm developed by Marquardt [12] was used. Although $\eta_o$ can be obtained from the data, it was treated as a fitting parameter to avoid biasing the fits with any transients which could have been present at the beginning of the anneal. If the initial viscosity obtained from the fit was too different from the measured one, indicating the presence of transients, the first few points of the run were deleted. Refitting the shortened data set then results in closer agreement between the fit and experimental values for $\eta_o$.

Figure 3 shows the viscosity increase in a $Pd_{77.5}Cu_6Si_{16.5}$ as-quenched ribbon, during isothermal annealing at 529K. For the entire length of the test, the plot is linear; it shows no evidence of saturation to a constant value. The temperature dependence of the slopes of these plots, $\dot{\eta}(T)$, is shown on the low temperature side of Fig. 4.

Figure 5 shows the viscosity increase for an as-quenched PdCuSi ribbon specimen at 615K. The viscosity increase is clearly non-linear, with $\dot{\eta}$ first decreasing as the equilibrium state is approached, and then increasing due to the onset of crystallization.

To determine the point at which crystallization effects were no longer negligible, an increasing fraction of each annealing data set was fit to the relaxation models. In a perfect isothermal annealing experiment, i.e., one in which the sample remained fully amorphous, the same set of fitting parameters

should be obtained regardless of the fraction of the test used. The point at which crystallization effects become significant is taken to be that at which $\eta_{eq}$ and $\chi^2$ begin to increase sharply from a reasonably constant value (see Fig. 6). $\chi^2$ is defined as the sum of the squared difference between the calculated and experimental elongation data.

In all the increasing viscosity experiments near $T_g$, the $\chi^2$ of the unimolecular fit was larger than that of the bimolecular one. Unlike the bimolecular $\chi^2$, which exhibited a reasonably constant value before rapidly increasing due to incipient crystallization, the unimolecular $\chi^2$ increased with increasing fraction of the data included in the fit. Figure 6 shows a plot of $\eta_{eq}$ and $\chi^2$ for the unimolecular and bimolecular fits as a function of the longest annealing time included in the fit, for the specimen in Fig. 5. For this specimen, appreciable crystallization was judged to occur after about 4 hours, based on the rapid departure from the reasonably constant initial value of $\eta_{eq}$. The value of $\eta_{eq}$ plotted in Fig. 14 was averaged from the $\eta_{eq}$ value between 2 and 4 hours of the run. It was assumed that for a given run the scatter in $\eta_{eq}$, with increasing fraction of the data (with no appreciable crystallization) included in the fit, is due to random errors. The error bar indicated in Fig. 14 was calculated as $(\eta_{eq}^{max} - \eta_{eq}^{min})/4$, and is assumed to be the standard deviation. From crystallization studies (discussed below), a few percent crystallinity is known to be present at 3 hours into the anneal. Figure 5 shows the fits obtained from the unimolecular and bimolecular models as light and heavy curves, respectively. Only the first three hours of the creep test were used for fitting. The bimolecular model fits the data very well whereas the unimolecular model does not, due to the fundamental difference in shape between the model viscosity curves. Figure 7 is an enlarged plot of the first three hours of Fig. 5. Figure 8 shows the model

fits to the original elongation data. For the fits shown, the unimolecular $\chi^2$ is 17 times larger than the bimolecular $\chi^2$. Figure 9 shows the viscosity increase for another specimen at 620K, again illustrating the superiority of the bimolecular fit.

We have also observed the isothermal approach to equilibrium in the reverse direction: a specimen, annealed for a long time at a low temperature (A → B on the schematic of Fig. 1), was brought rapidly to a temperature beyond the equilibrium curve (B → C on Fig. 1) and the viscosity decrease was observed (C → E on Fig. 1). Figure 10 shows the viscosity decreasing for a specimen first annealed at 591K for 2 days before being brought to 615K at a heating rate of 24K/min. The viscosity eventually increases due to crystallization. The data before crystallization can be fit very well using either the unimolecular or bimolecular model. For the first 0.64 hours of the data, the unimolecular $\chi^2$ is 1.01 times the bimolecular $\chi^2$. Both fits give nearly the same asymptotic value for $\eta_{eq}$ that is also in excellent agreement with the asymptotic value obtained from the bimolecular fit to increasing viscosity, as shown in Figs. 11 and 12. Note that the apparent viscosity decrease is faster for the decreasing viscosity case. The same difference has been observed by Lillie in his viscosity measurements on soda-lime glass [10].

Figure 13 shows the viscosity behavior for a specimen first annealed at 594K for 164 hours before being brought to 608K. The apparent viscosity remained constant before eventually increasing due to crystallization. The constant viscosity value was taken to be $\eta_{eq}$.

The bimolecular rate constants, $k_2$, obtained from fits to the increasing viscosity data are plotted in Fig. 4 together with $\dot{\eta}$ (constant) values obtained by creep and stress relaxation measurements [3]. For $\eta_{eq} \gg \eta(t)$, $k_2 = \dot{\eta}$. Note that $k_2$ has a non-Arrhenian temperature dependence. This

behavior has also been observed in $Fe_{40}Ni_{40}P_{14}B_6$ by Taub and Luborsky [3].

### 3.3 Effect of Crystallization

The viscosity change as a result of structural relaxation and crystallization was fit to the Einstein equation for the viscosity, $\eta_{eff}$, of a mixture consisting of a small volume fraction, $f_c$, of spherical particles suepended in a medium of viscosity $\eta$ [13]:

$$\eta_{eff} = \eta(1 + 2.5f_c) \tag{10}$$

The crystals were assumed to grow spherically with a constant growth rate, v, from randomly positioned nuclei. The Johnson-Mehl-Avrami analysis [14] for isothermal nucleation and growth then predicts:

$$f_c(t) = 1 - \exp(- at^3) \tag{11}$$

where $a = N(4/3)\pi v^3$; N = concentration of nuclei.

The dashed curves in Figs. 5 and 10 are the fits to the data, treating a as a new fitting parameter in combination with the previously found bimolecular values for $\eta_{eq}$, $\eta_o$ and $k_2$. The calculated crystalline volume fraction at the end of each of the tests in Figs. 5 and 10 was 0.46 and 0.13 respectively, in reasonable agreement with direct observation by metallography.

Metallography also revealed that crystallization in these specimens originated from the specimen surface. However, a model based on planar growth of the crystalline phase and the same strain rates for the amorphous and crystalline phases cannot adequately fit the data [15,16]. The remarkable fit

of equation 10 despite the non-random arrangement of non-spherical crystals, is probably due to effectively treating the geometrical factor 2.5 as part of a fit parameter, since it appears as a product with $f_c$.

Patterson and Jones [17] also found excellent agreement between the creep rate measured during crystallization of $Fe_{40}Ni_{40}P_{14}B_6$ and those predicted by eq. 10 up to at least 30% crystalline volume fraction. In their study, the specimen was assumed to be at equilibrium with $\eta_{eq}$ equal to the initial viscosity. The change in the crystalline volume fraction was calculated from the calorimetrically measured crystallization exotherm of the same material.

## 4. TEMPERATURE DEPENDENCE OF THE METASTABLE EQUILIBRIUM VISCOSITY

Figure 14 summarizes the $\eta_{eq}$ values from 608K to 630K which were obtained in either of three ways: (1) from the bimolecular fits to the increasing viscosity data, (2) from the averaged $\eta_{eq}$ values from the bimolecular and unimolecular fits to decreasing viscosity data, and (3) directly measured values from experiments of the type shown in Fig. 12. The results of the fits to an Arrhenius equation $\eta = A \exp(B/T)$, Fulcher-Vogel equation $\eta = A \exp(B/(T-T_o))$, and ''hybrid'' equation $\eta = A \exp(B/(T-T_o)) \exp(C/T)$ are also shown. The Fulcher-Vogel and ''hybrid'' equations describe the data well, whereas the Arrhenius equation does not. The best-fit Fulcher-Vogel curve has $A = (1.20 \pm 0.4)\times10^8$ $Nsm^{-2}$, $B = 338 \pm 20K$, $T_o = 583.4 \pm 1K$. The additional parameter introduced in the ''hybrid'' equation does not improve the fit significantly: its $\chi^2$, normalized for the number of fit parameters, is higher than that of the Fulcher-Vogel equation. Also shown in Fig. 14 are earlier measurements of the equilibrium viscosity reported by Chen and Goldstein [8] for the same alloy.

## 5. DISCUSSION

The creep elongation data were fit to predictions of unimolecular and bimolecular annihilation or creation of defects responsible for flow. It was found that the bimolecular model described the viscosity increase during relaxation best.

One may ask whether first- or second-order rate equations in the viscosity departure from equilibrium:

$$\frac{d\eta}{dt} = - k_4(\eta_{eq}-\eta)^{1 \text{ or } 2} \tag{12}$$

might not describe the data just as well. It turns out that a second-order equation in $(\eta_{eq}-\eta)$ results in an equation identical to the bimolecular defect-based one, whereas a first-order equation in $(\eta_{eq}-\eta)$ results in an equation identical to equation (7).

In amorphous covalently bound systems, such as soda-lime glass [10], the viscosity increase during relaxation has also been shown to be described best by the bimolecular model. Density and refractive index studies above the fictive temperature have shown essentially unimolecular kinetics, with deviations in the early states [11]. In these systems, which are modeled as continuous random networks, the flow defects are easily identified as broken bonds which allow shear rearrangements. Since annihilation of these bonds occurs when two of them come together to form a covalent bond, the bimolecular kinetic law of equation (3) is expected to apply to the viscosity increase. Since formation of a pair of broken bonds only requires a single bond to come apart, the unimolecular kinetic law of equation (2) is expected to apply to relaxation above the fictive temperature.

For the metallic glasses, one can only speculate about the nature of the microscopic mechanism that accounts for the bimolecular kinetics during the viscosity increase [18]. Since the chemical short range order in metal-metalloid glasses such as PdCuSi is very strong, one can construct a direct equivalent to the broken bond mechanism in covalent systems. Diffraction evidence shows that the metalloid (X) atoms are, ideally, surrounded by metal(M) atoms only [19]. Direct analogues to broken covalent bonds would be chemical defects, i.e.: X-X neighbors and complementary excess M-M neighbors, provided these can be shown to govern flow.

It is also possible to construct purely topological bimolecular annihilation mechanisms. In that case a flow defect is a cluster of atoms which undergoes a shear rearrangement upon a density or free volume fluctuation, resulting in a local shear strain that is transferred elastically to the specimen boundary. The free volume fluctuation, and hence a flow defect, can only be eliminated at a special site or ''relaxation defect'', which is a cluster of atoms, wherein as a result of a free volume fluctuation, atoms rearrange and transfer at least part of this free volume out to the specimen boundary. Any rearrangement with a dilatational component can be such a relaxation defect [9]. The ''p/n defects'' proposed by Egami et al. [20] may be an example of these defects, provided they can be shown to produce flow.

Another pair of topological defects can be defined using Nelson's model for the glassy state, in which a perfect tetrahedral packing on the surface of a four-dimensional sphere is mapped into flat three-dimensional space by the introduction of an array of disclinations [21]. Most of these disclination lines are long and intertwined and hence kinetically frozen. Vacancies or interstitials in the four-dimensional array, however, correspond to localized

disclination ''bubbles'' of opposite sign that can mutually annihilate [22]. Again, if these ''bubbles'' can be shown to produce local shear, their annihilation may explain the bimolecular relaxation kinetics.

Since fitting our decreasing viscosity data to the bimolecular and unimolecular equations could not distinguish between the two models, speculation on the mechanisms for generation of flow defects would be premature. Further measurements on an even more stable glass, such as $Pd_{40}Ni_{40}P_{20}$, are underway to resolve this.

The newly determined values of $\eta_{eq}$ are well described by the Fulcher-Vogel and ''hybrid'' equations, but not by the Arrhennius equation. This result is expected in metallic glasses where the flow process requires a cooperative motion involving a number of atoms. The Fulcher-Vogel equation is also the one predicted by the free volume [23] and configurational entropy models [24]. In contrast, the equilibrium viscosity behavior in systems such as pure silica where flow is largely due to bond-breaking exhibits Arrhenian behavior. Van den Beukel and Radelaar [25] advocate using the ''hybrid'' equation to describe the equilibrium viscosity in metallic glasses in order to account for the rather high apparent activation energies observed in isoconfigurational flow experiments [1]. They pointed out that Chen and Goldstein's results [8] can be equally well described by the Fulcher-Vogel and ''hybrid'' equations. Moreover, by fixing the fit parameter C (see Section 4) at different values they also showed that the Chen and Goldstein data can be equally well described by different sets of ''hybrid'' fit parameters. The effect of the additional fitting parameter contained in the ''hybrid'' equation was to lower the $\chi^2$ in the fit to our data. However, the normalized $\chi^2$ for the Fulcher-Vogel fit remained the lowest.

The value of $T_o$ for the Fulcher-Vogel fit to our data is similar to that

found by Chen and Goldstein. The parameter B, however, is considerably smaller. (338K vs. 3180K); according to the free volume model, with a volume thermal expansion coefficient of $4.5 \times 10^{-5} K^{-1}$ [26], our value of B corresponds to a critical free volume fluctuation, $v^*$, of only 6% of the atomic volume. The pre-exponential, A, in our fit is very large. Extrapolation of the equation to higher temperatures gives unphysically high values for the viscosity, and is therefore unwarranted. This is not unusual, however, since it is known that for most amorphous systems, metallic and non-metallic ones, a single set of Fulcher-Vogel parameters is inadequate to describe the viscosity over the entire temperature range.

Our values of $\eta_{eq}$ are clearly higher than those measured by Chen and Goldstein [8], by almost an order of magnitude. Since the previous authors assumed that the equilibrium structure was attained shortly after the decay of the anelastic transients, and since the earlier values were not confirmed by decreasing viscosity relaxation, the discrepancy is probably due to insufficient relaxation in the earlier experiments.

The data for $\eta_{eq}$ plotted in Fig. 14 only span the temperature range from 608 to 630K. Increasing viscosity experiments were also performed outside this range. At higher temperatures, crystallization occurred too rapidly. At slightly lower temperatures, crystallization was delayed, but still occurred prior to the decay of the anelastic transient. Since anelastic transients decay more rapidly at higher temperatures, several tests were performed whereby the specimen is first annealed at a slightly higher temperature than the testing temperature for a short period of time. These attempts were unsuccessful, however, in sufficiently delaying crystallization, probably due to enhanced devitrification at the pre-annealing temperature. It should be noted that the $\eta_{eq}$ values at the two lowest temperatures were obtained from

experiments that consisted of an initial long pre-anneal at a low temperature prior to rapid warming to final testing temperature. This latter procedure was effective probably because during the pre-anneal anelastic transient decay was completed with little accompanying crystallization due to the low temperature, and high initial viscosity at the final temperature helped retard the growth of the crystalline phase. At still lower temperatures, the viscosity increase was linear over the entire duration of the test.

## 6. CONCLUSIONS

The viscosity increase as a result of structural relaxation was observed to be linear in time at temperatures well below $T_g$, but non-linear at temperatures near $T_g$, when the glass is closer to equilibrium. The viscosity increase could be described best by a mechanism involving bimolecular annihilation of chemical or topological flow defects. The viscosity decrease as a result of structural relaxation from above the equilibrium value was also measured and found to be fit adequately by both unimolecular and bimolecular models for creation of flow defects.

New values of the equilibrium viscosity of $Pd_{77.5}Cu_6Si_{16.5}$ were obtained in three ways: (1) from the asymptotic value of the bimolecular viscosity fit to increasing viscosity data, (2) from the averaged asymptotic values of bimolecular and unimolecular viscosity fits to the viscosity decreasing data, and (3) from direct measurements on specimens previously well-annealed at a lower temperature. Within experimental accuracy, the same asymptotic value for $\eta_{eq}$ is obtained from fits to increasing and decreasing viscosity data at the same temperature. The newly determined values of $\eta_{eq}$ are about an order of magnitude higher than the literature data for the same alloy. They are

well described by the Fulcher-Vogel equation.

The effect of partial crystallization on the viscosity could be described by a simple modification of the Einstein theory for flow of dispersions.

## ACKNOWLEDGMENTS

We thank K.F. Kelton for the use of his fitting program. This work has been supported by the Office of Naval Research, Contract N00014-77-C-0002.

## FIGURE CAPTIONS

Figure 1. Shear viscosity $\eta$ in the various stability regimes: stable equilibrium above $T_M$, metastable equilibrium, isoconfigurational (BC), structural relaxation (AB, DE, CE).

Figure 2. Total strain and apparent viscosity changes as a result of both structural relaxation and delayed elasticity after loading and unloading of the specimens.

Figure 3. Example of linear viscosity increase with time for $Pd_{77.5}Cu_6Si_{16.5}$ at T = 529K.

Figure 4. Arrhenius plot of the rate constants $k_2$ or $\dot{\eta}$ (constant) determined from stress relaxation and creep experiments.

Figure 5. Example of the nonlinear viscosity increase of a PdCuSi ribbon specimen at 615K. The fits to the unimolecular and bimolecular models are shown.

Figure 6. $\eta_{eq}$ and $\chi^2$ obtained by fitting the data shown in Fig. 5 to the unimolecular (open symbols) and bimolecular (solid symbols) models as a function of the longest annealing time included in the fit.

Figure 7. Enlarged plot of the bimolecular and unimolecular fits to the first three hours of the data in Figure 5. The bimolecular model is a better fit to the data than the unimolecular model. The fundamental difference in shape between the model curves is clear.

Figure 8. The bimolecular and unimolecular fits to the first three hours of the original elongation data in Fig. 5. The bimolecular model fits the data better than the unimolecular model.

Figure 9. Example of the non-linear viscosity increase for a $Pd_{77.5}Cu_6Si_{16.5}$ ribbon specimen at 620K. The light and heavy curves are the fits

to the unimolecular and bimolecular models, respectively.

Figure 10. Example of the viscosity decrease with time during isothermal annealing of PdCuSi at 615K, above the fictive temperature. The specimen was preannealed at 591K for 74 hours. The light and heavy curves are the unimolecular and bimolecular fits to the data, respectively. The dashed curve takes into account crystallization.

Figure 11. Viscosity relaxation of two PdCuSi specimens at 612K. The upper curve is for a specimen preannealed at 595K for 49 hours; the lower curve is for an as-quenched specimen. The fits to the decreasing and increasing $\eta$ give the same asymptotic value for $\eta_{eq}$.

Figure 12. Viscosity relaxation of two PdCuSi specimens at 615K. The upper curve is for the specimen in Figure 10; the lower curve is for an as-quenched specimen. The fits to the decreasing and increasing $\eta$ give the same asymptotic value for $\eta_{eq}$.

Figure 13. Viscosity change with annealing time at 608K for a PdCuSi ribbon specimen preannealed at 594K for 164 hours. The viscosity remained constant for several hours prior to specimen crystallization.

Figure 14. Summary of $\eta_{eq}$ values determined from model fits to increasing viscosity data (circles), decreasing viscosity data (dots), and direct measurements on specimens preannealed at low temperature (circled x). The temperature dependence of $\eta_{eq}$ is described well by the Fulcher-Vogel and ''hybrid'' equations. The Chen and Goldstein results are from ref. 8.

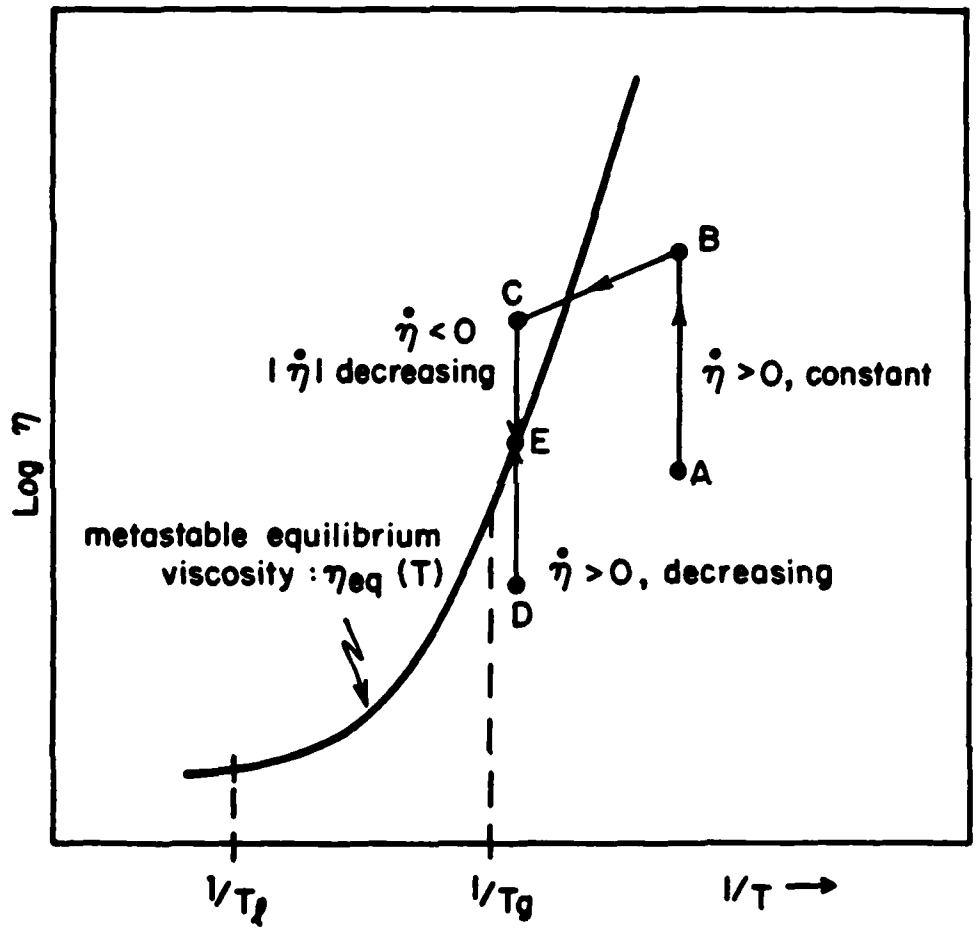


Figure 1

Shear viscosity η in the various stability regimes: stable equilibrium above $T_M$, metastable equilibrium, isoconfigurational (BC), structural relaxation (AB,DE,CE).

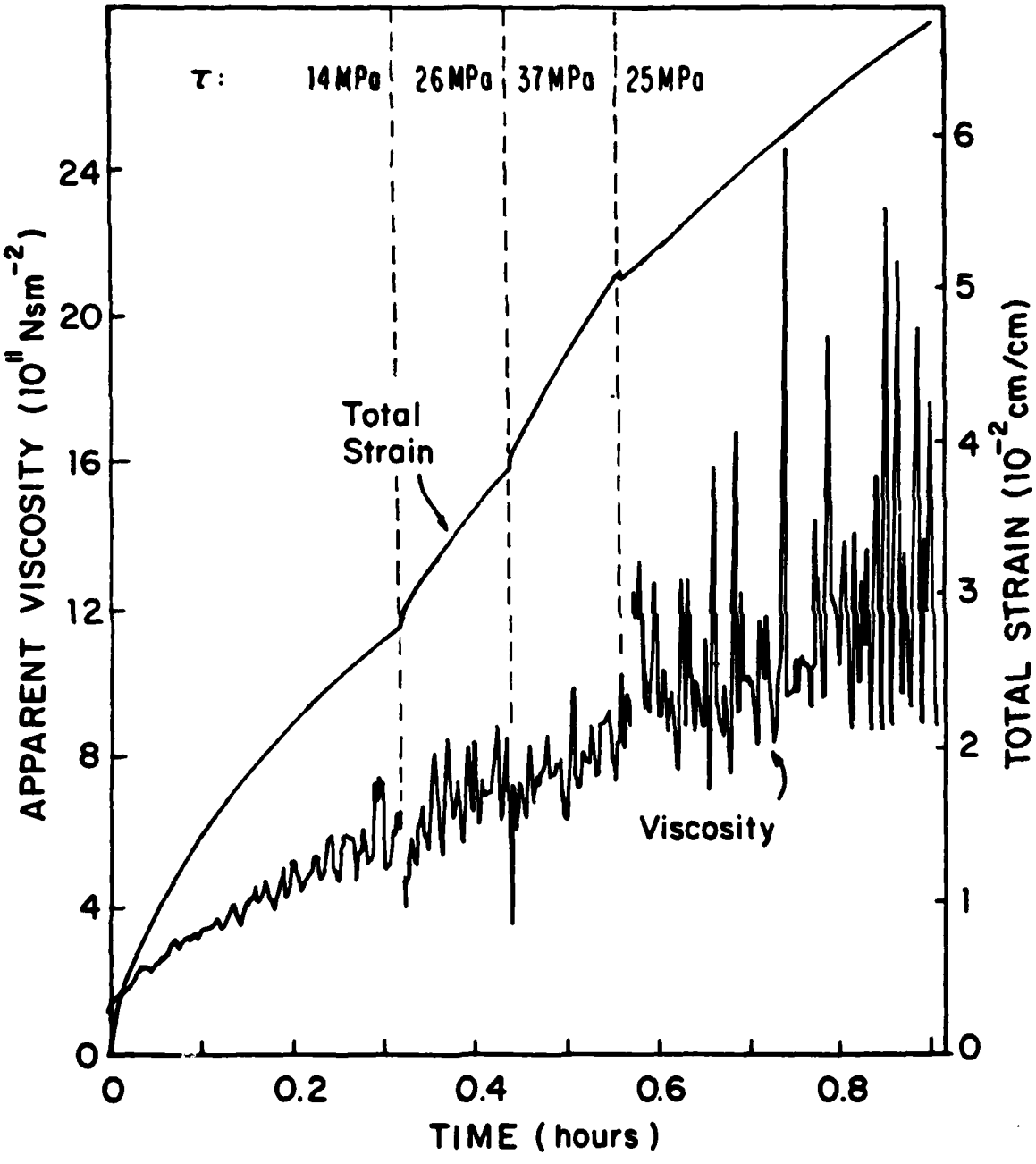


Figure 2

Total strain and apparent viscosity changes as a result of both structural relaxation and delayed elasticity after loading and unloading of the specimens.

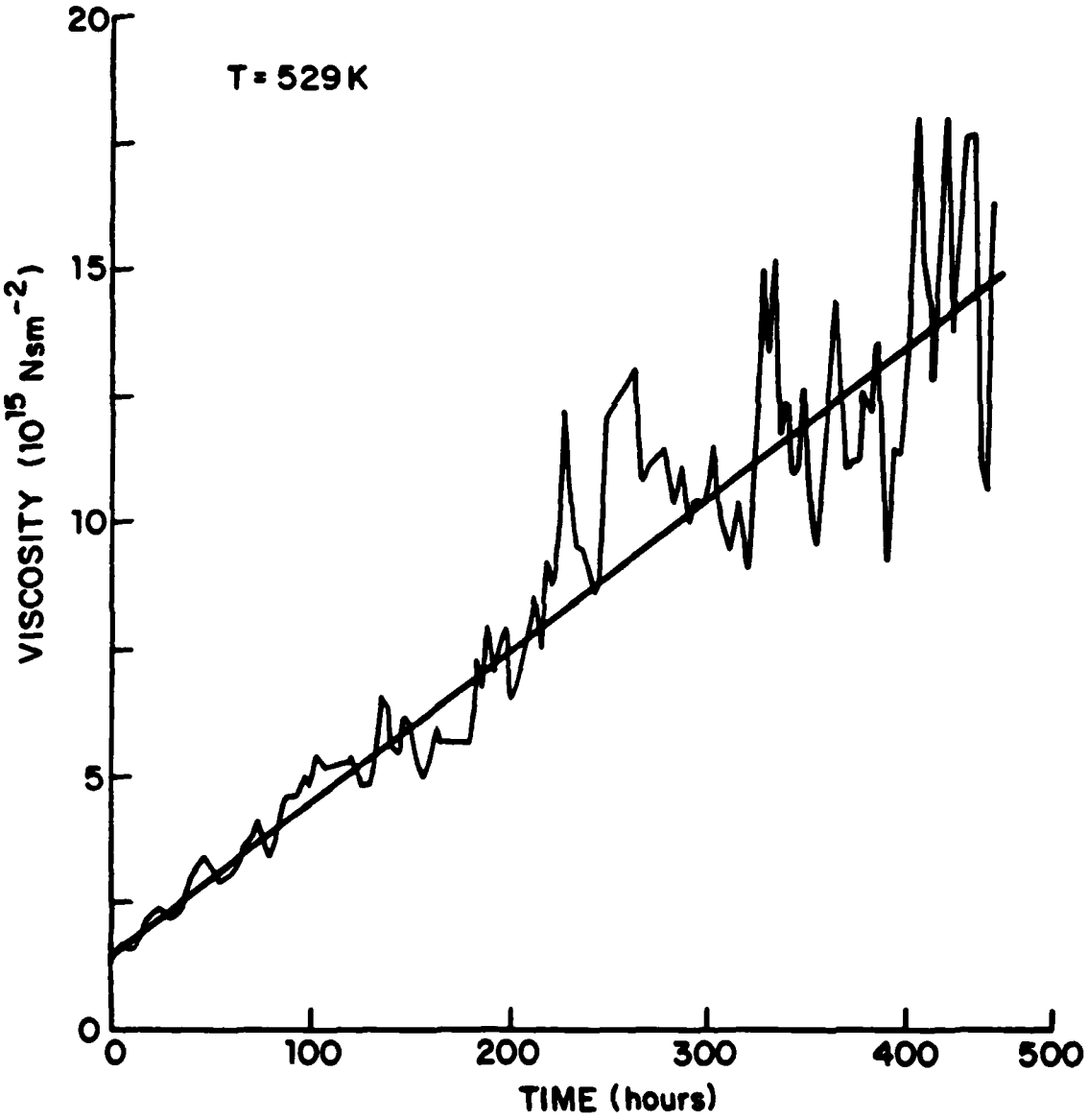


Figure 3

Example of linear viscosity increase with time for $Pd_{77.5}Cu_6Si_{16.5}$ at T = 529K.

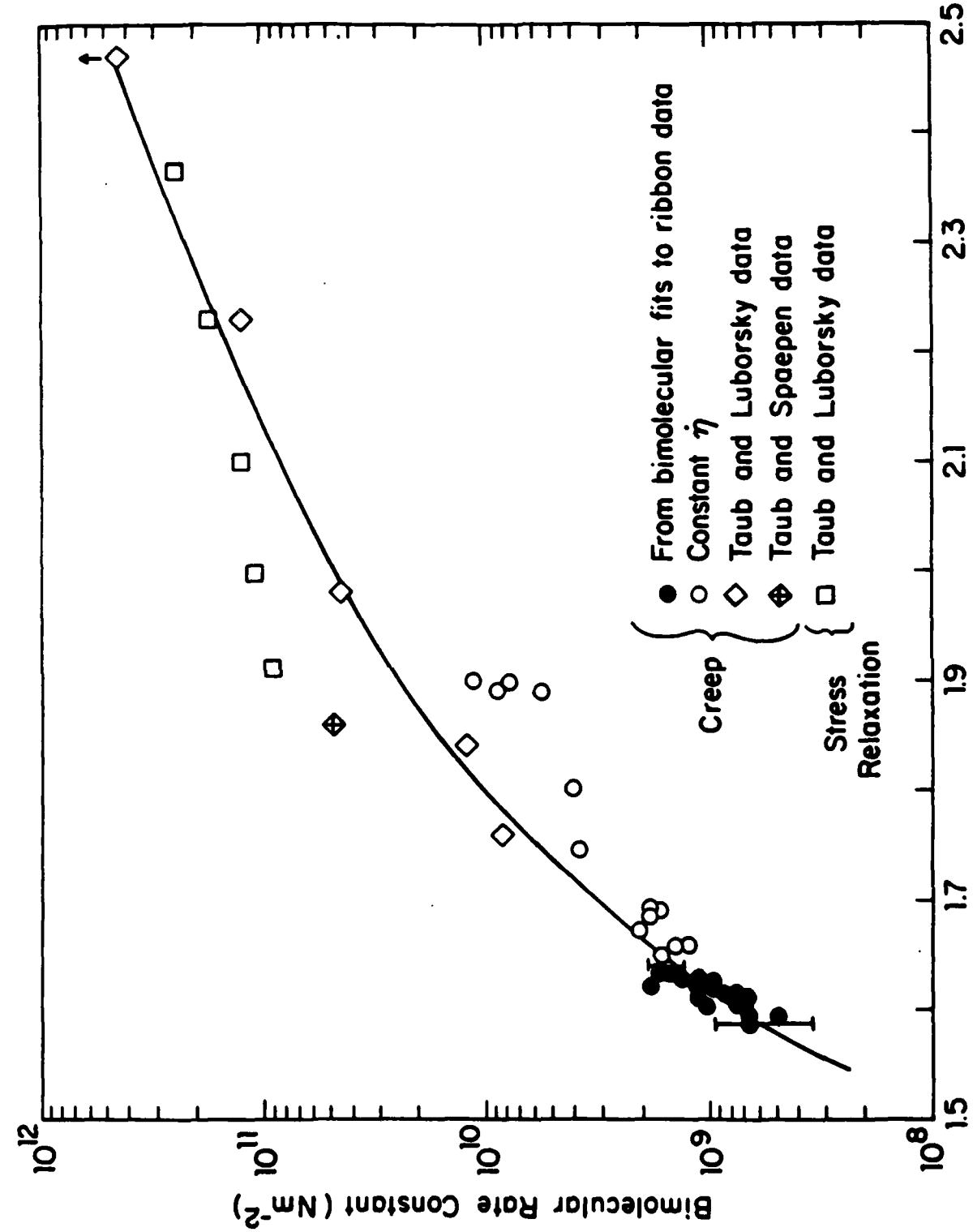


Figure 4

Arrhenius plot of the rate constants $k_2$ or $\dot{\eta}$ (constant) determined from stress relaxation and creep experiments.

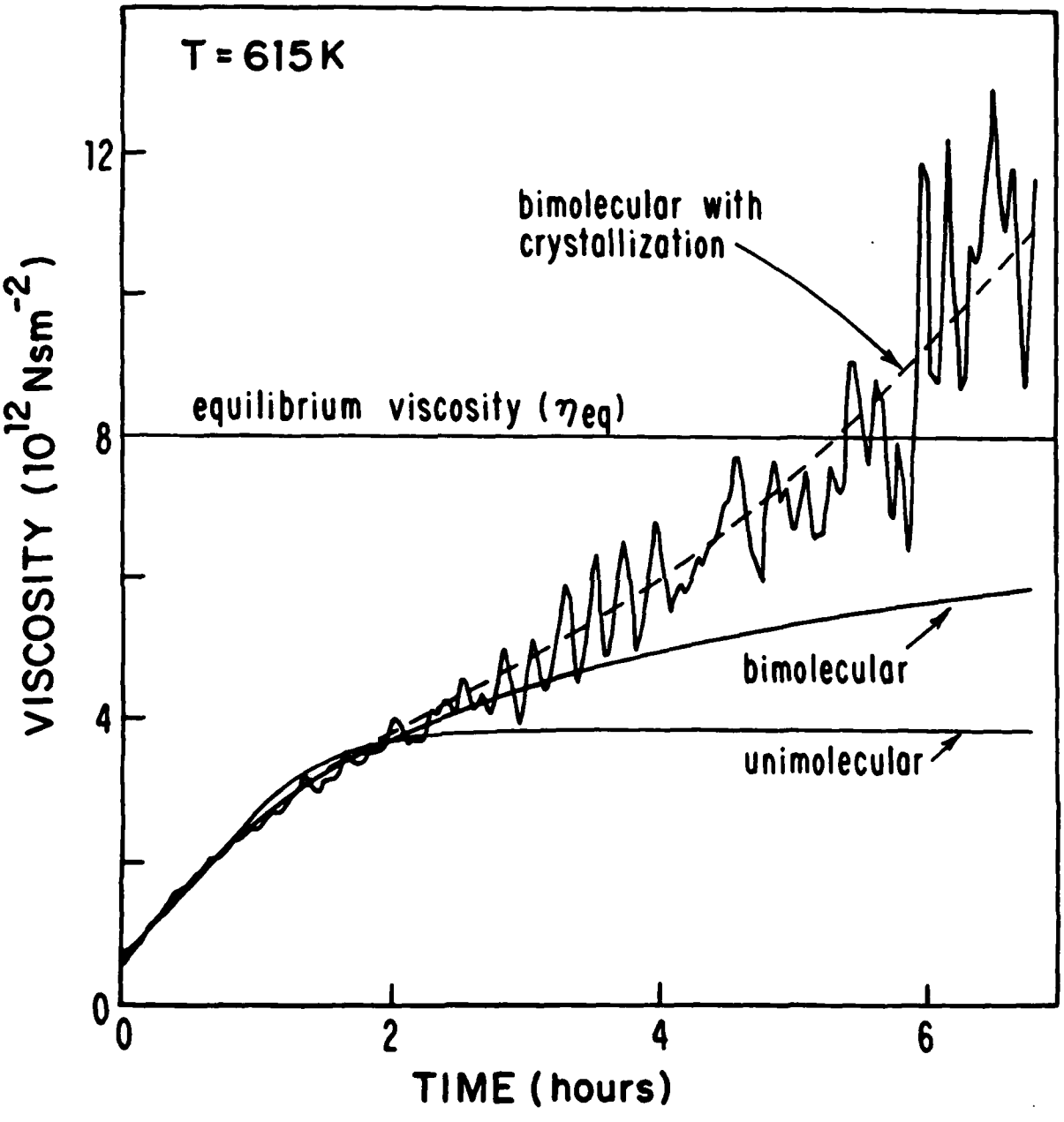


Figure 5

Example of the nonlinear viscosity increase of a PdCuSi ribbon specimen at 615K. The fits to the unimolecular and bimolecular models are shown.

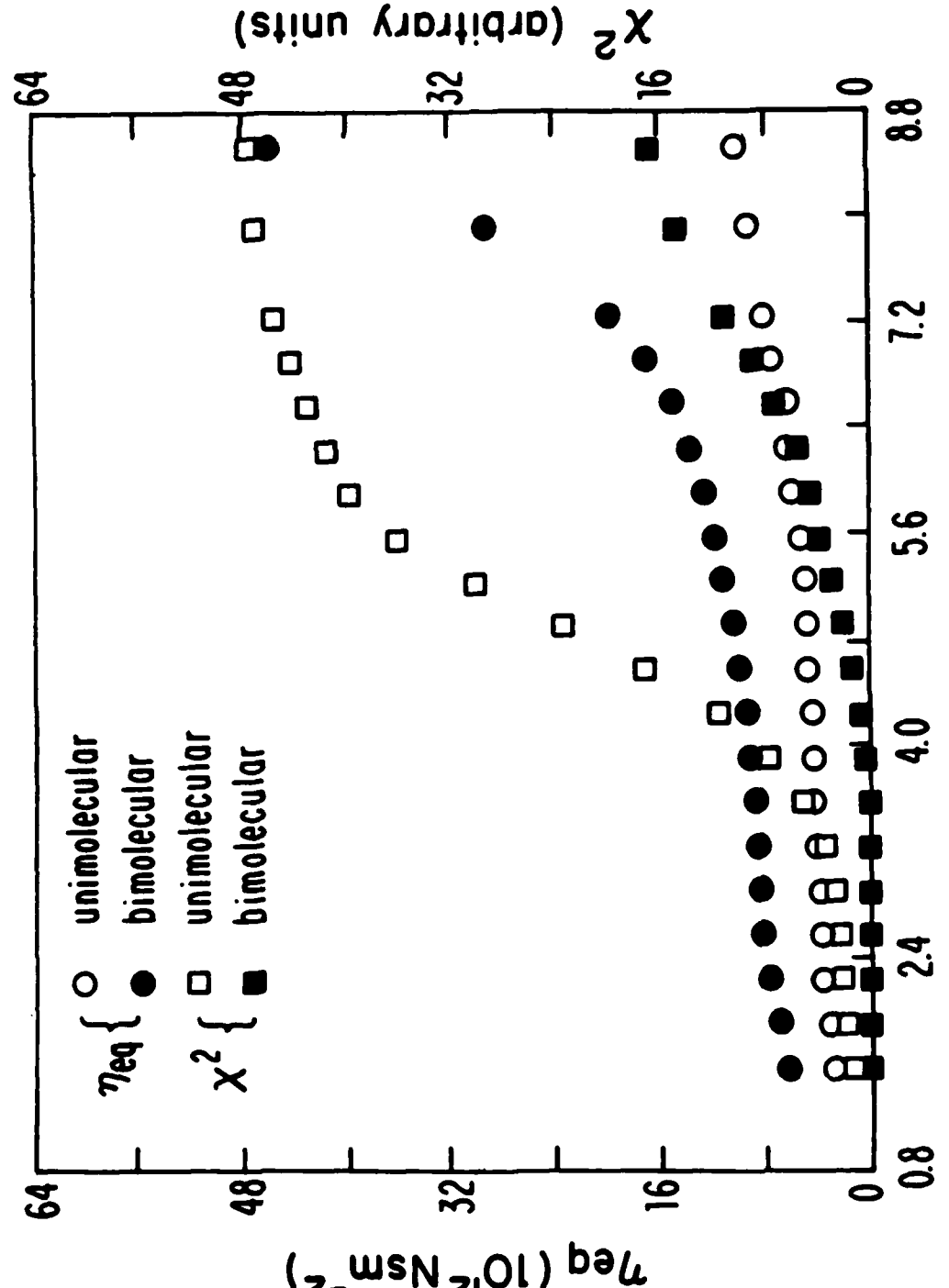


Figure 6

$\eta_{eq}$ and $\chi^2$ obtained by fitting the data shown in Figure 5 to the unimolecular (open symbols) and bimolecular (solid symbols) models as a function of the longest annealing time included in the fit.

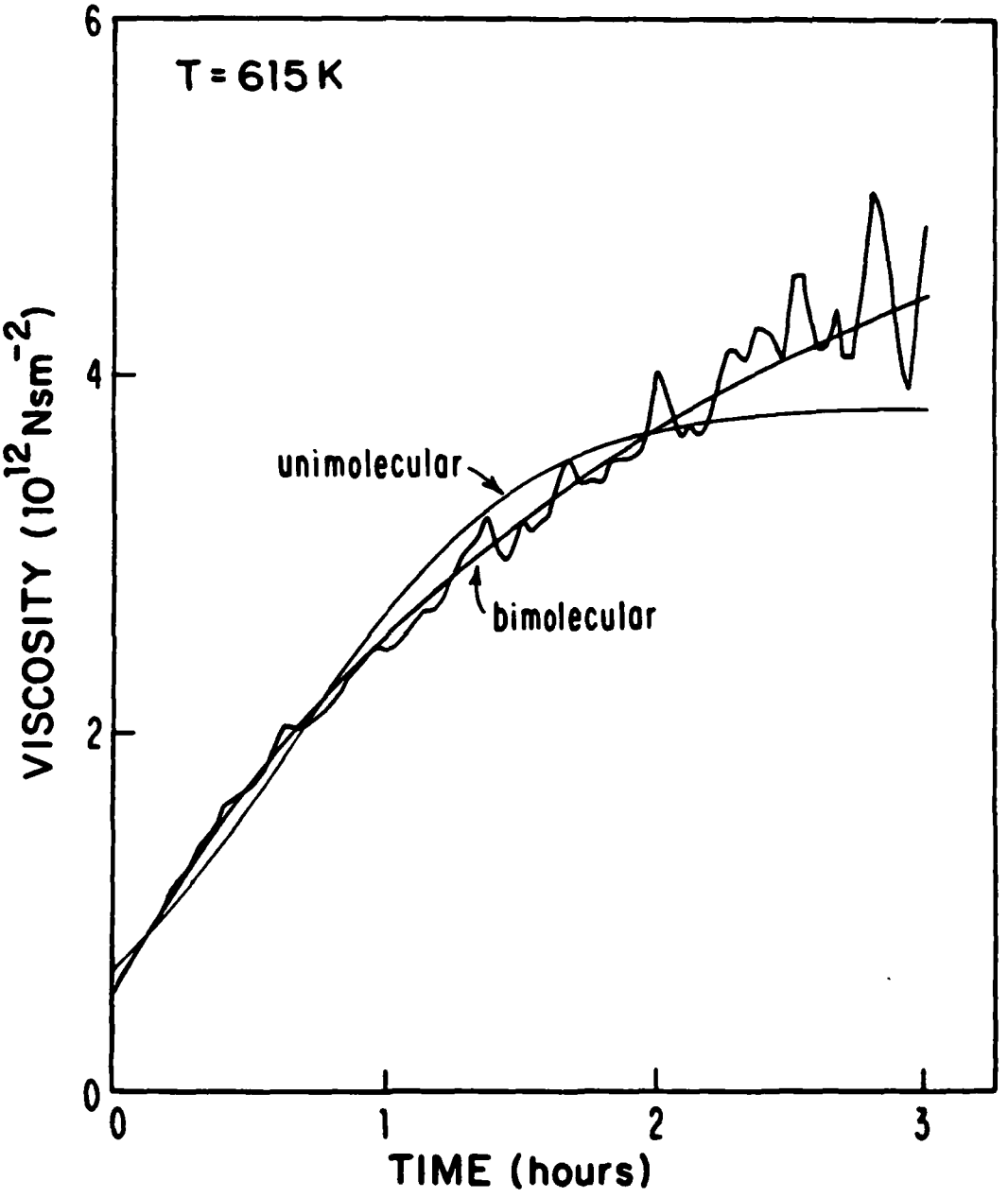


Figure 7

Enlarged plot of the bimolecular and unimolecular fits to the first three hours of the data in Figure 5. The bimolecular model is a better fit to the data than the unimolecular model. The fundamental difference in shape between the model curves is clear.

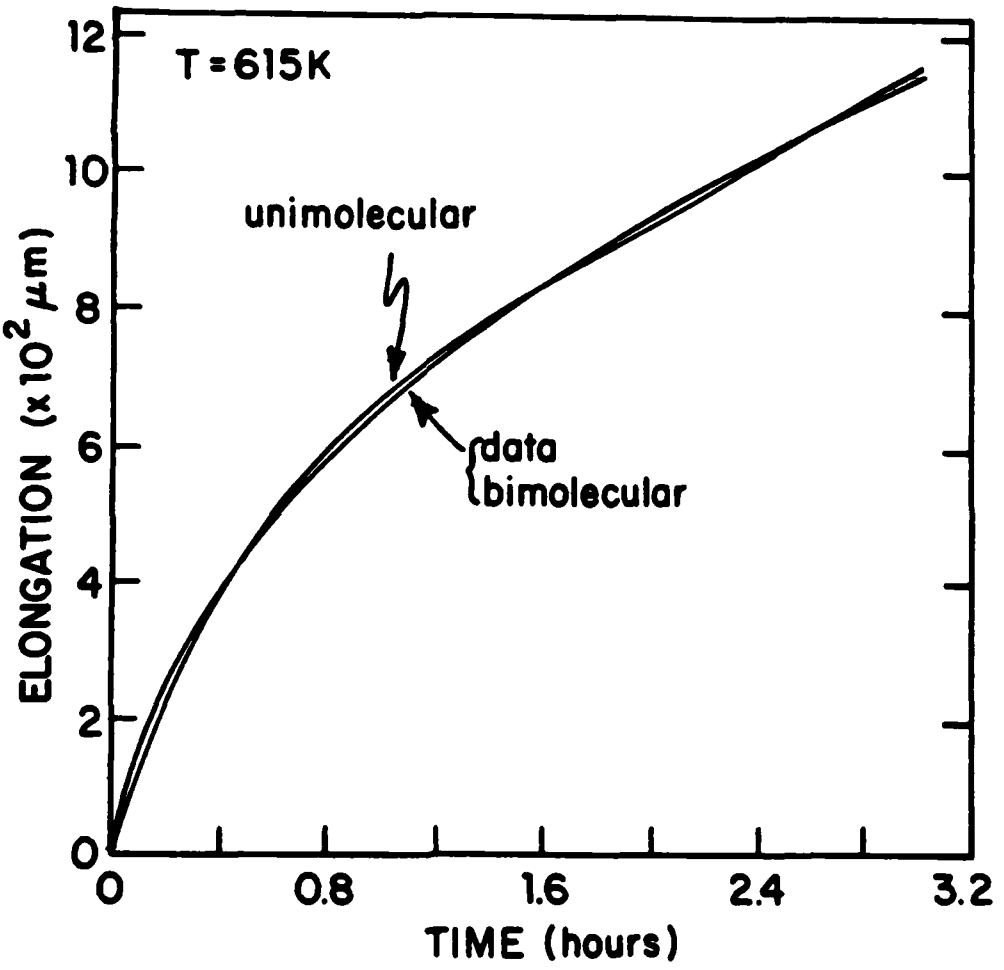


Figure 8

The bimolecular and unimolecular fits to the first three hours of the original elongation data in Figure 5. The bimolecular model fits the data better than the unimolecular model.

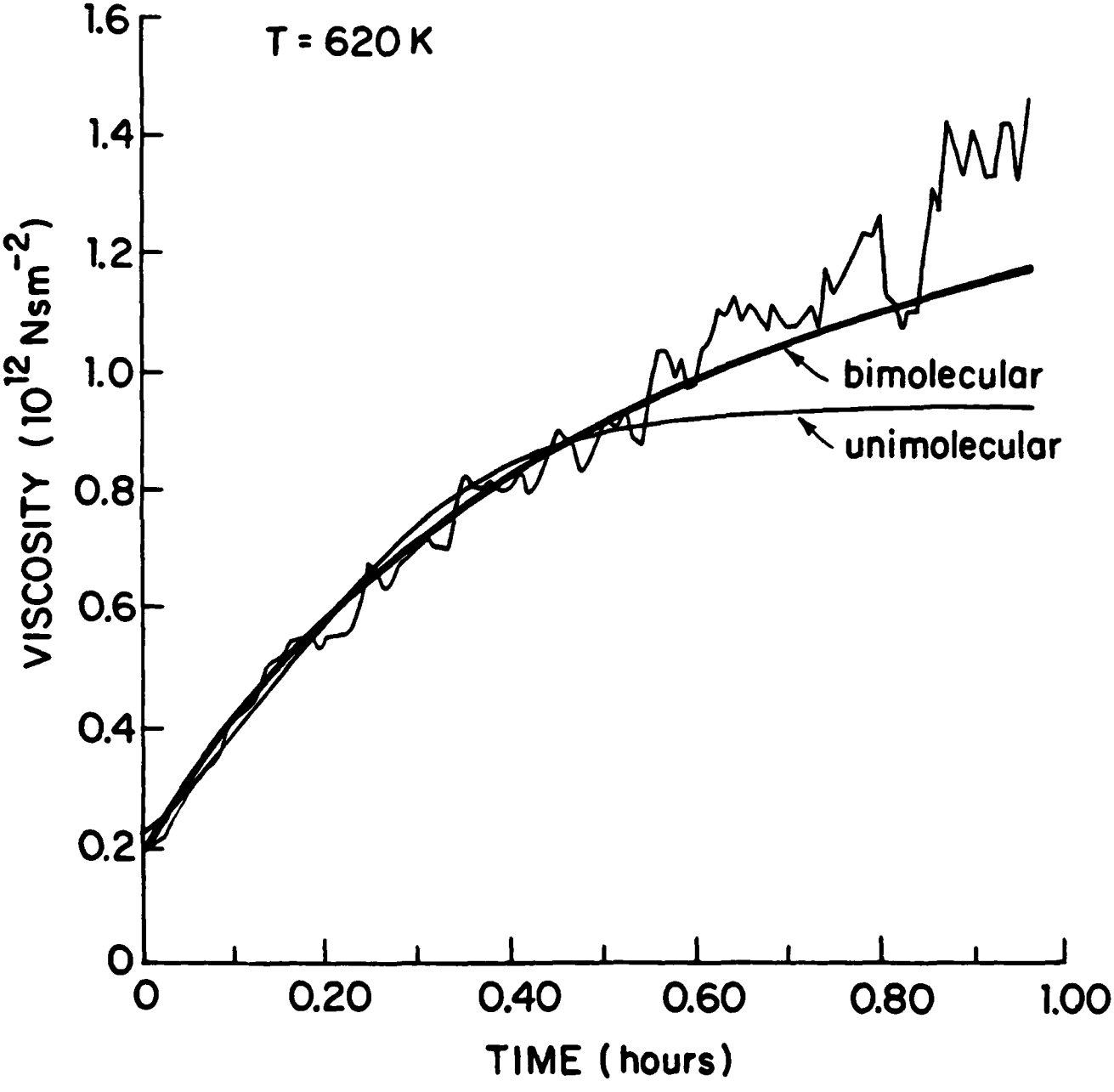


Figure 9

Example of the non-linear viscosity increase for a $Pd_{77.5}Cu_6Si_{16.5}$ ribbon specimen at 620K. The light and heavy curves are the fits to the unimolecular and bimolecular models, respectively.

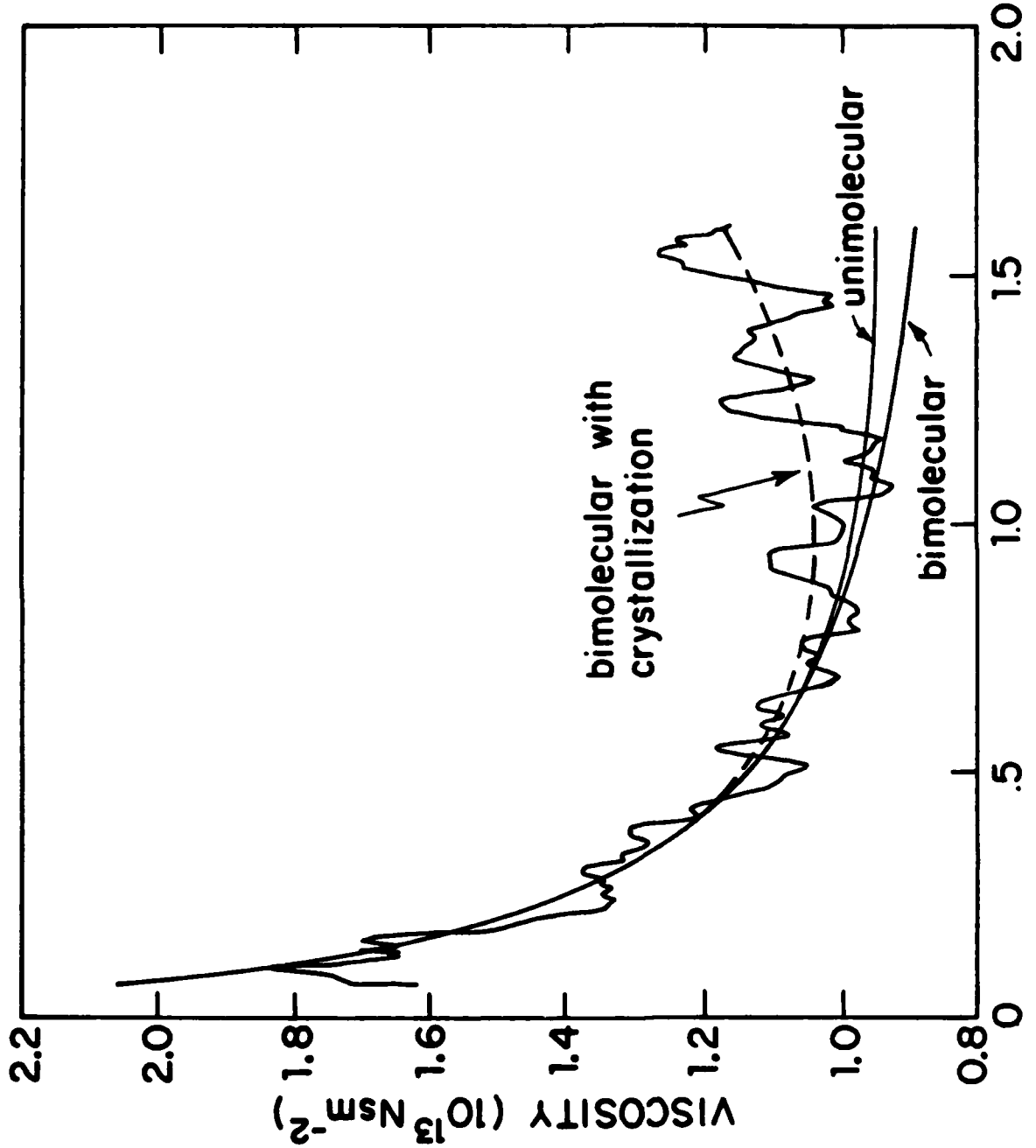


Figure 10

Example of the viscosity decrease with time during isothermal annealing of PdCuSi at 615K, above the fictive temperature. The specimen was preannealed at 591K for 74 hours. The light and heavy curves are the unimolecular and bimolecular fits to the data, respectively. The dashed curve takes into account crystallization.

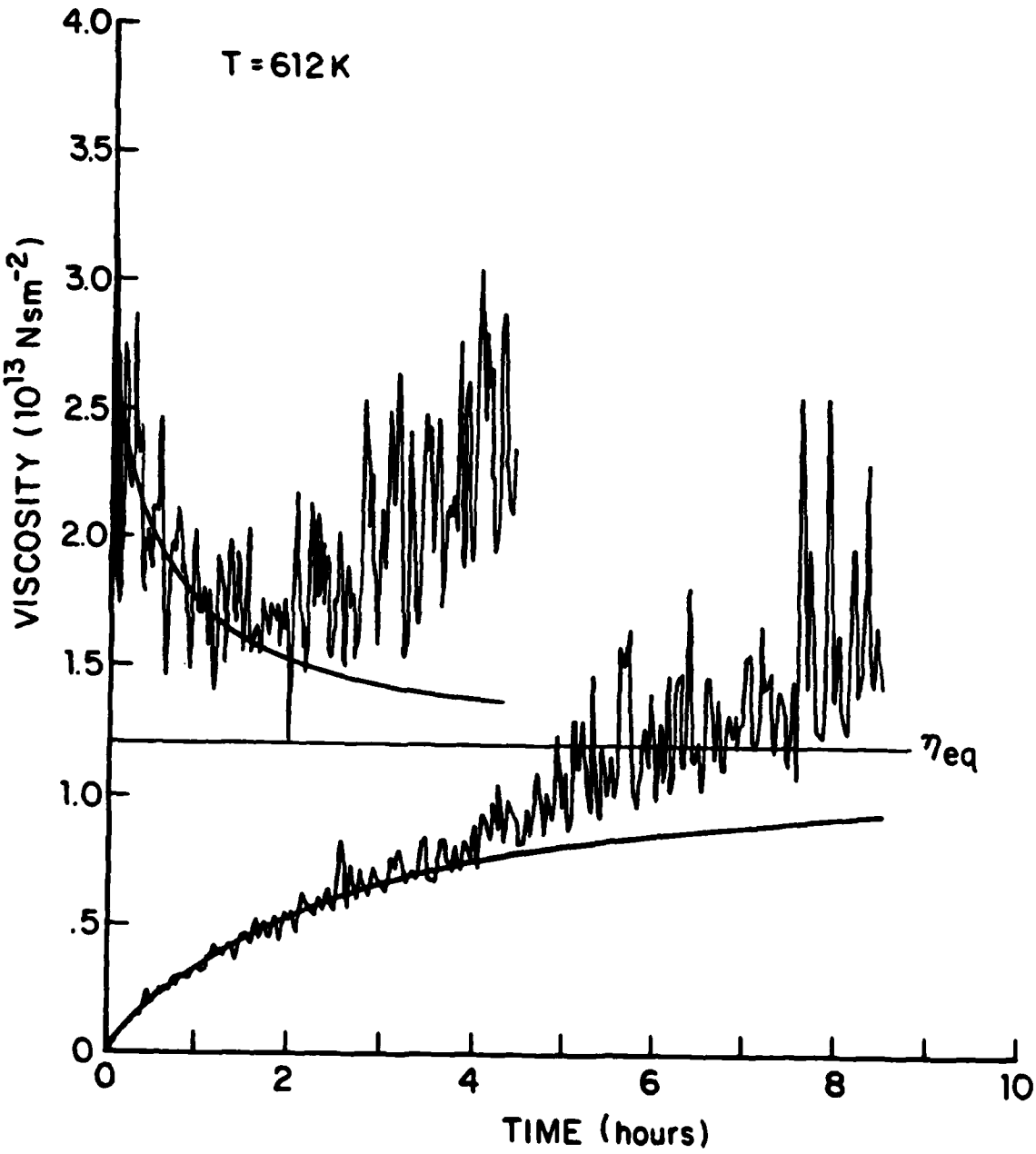


Figure 11

Viscosity relaxation of two PdCuSi specimens at 612K. The upper curve is for a specimen preannealed at 595K for 49 hours; the lower curve is for an as-quenched specimen. The fits to the decreasing and increasing $\eta$ give the same asymptotic value for $\eta_{eq}$.

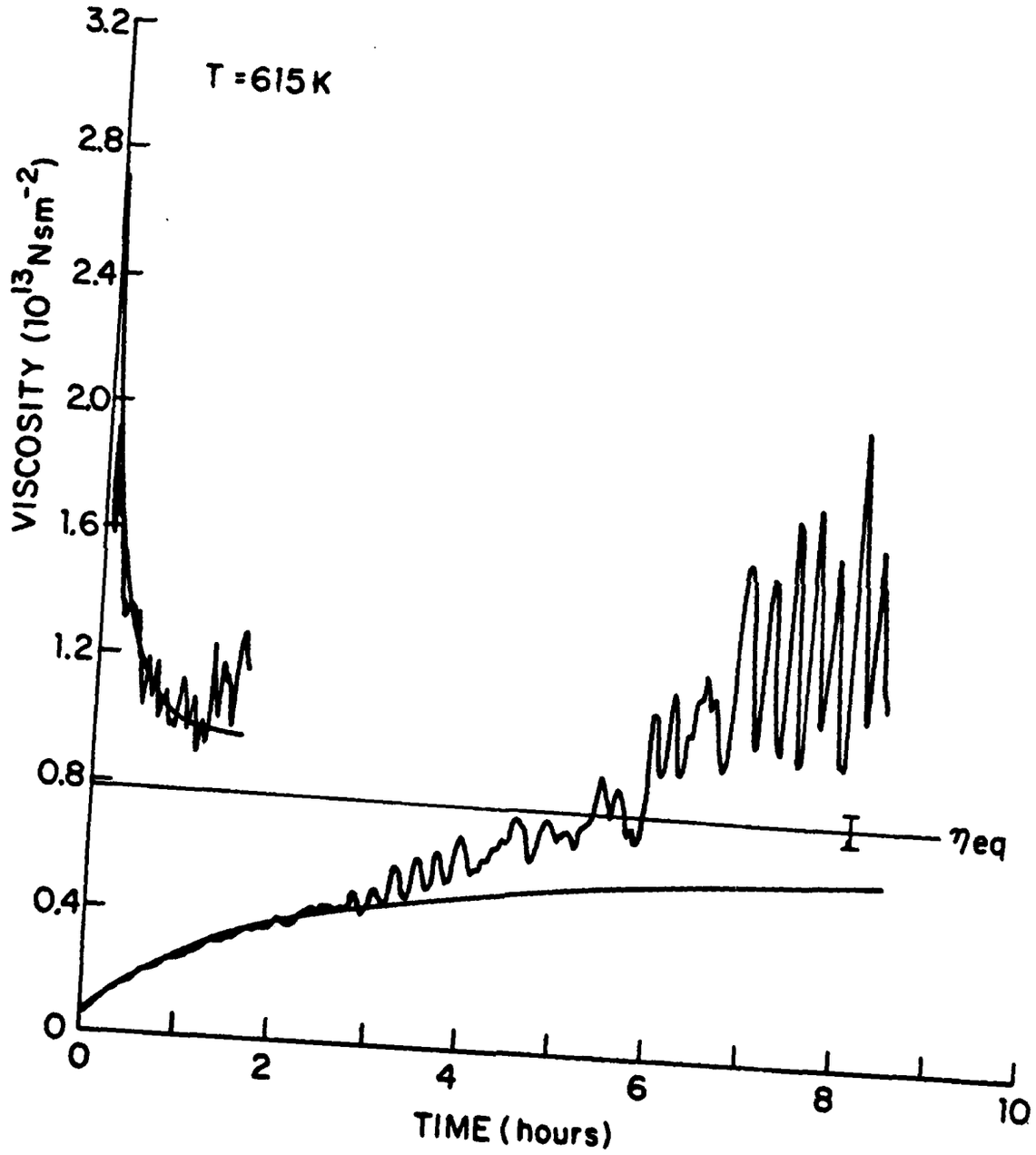


Figure 12

Viscosity relaxation of two PdCuSi specimens at 615K. The upper curve is for the specimen in Figure 10; the lower curve is for an as-quenced specimen. The fits to the decreasing and increasing $\eta$ give the same asymptotic value for $\eta_{eq}$.

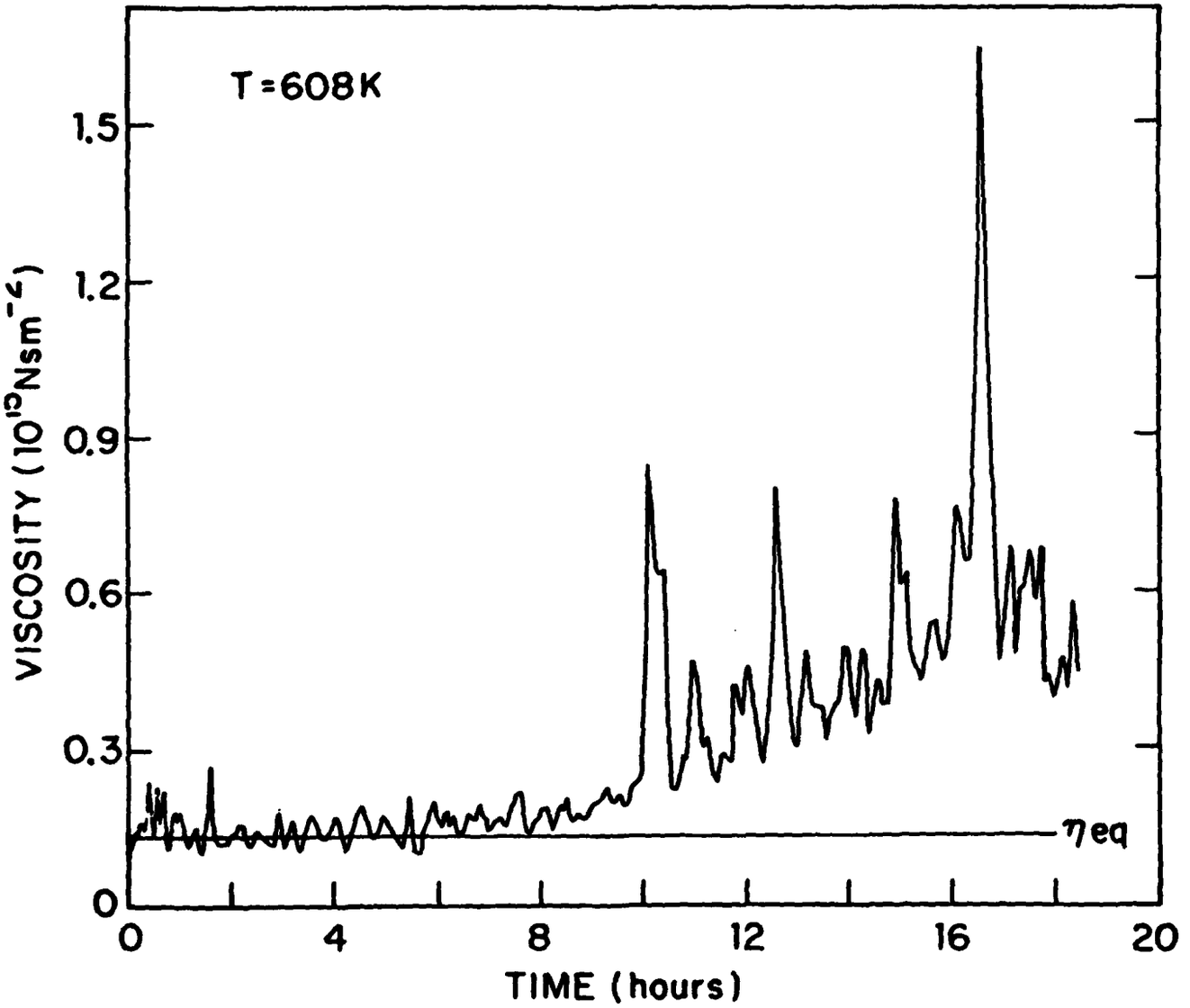


Figure 13

Viscosity change with annealing time at 608K for a PdCuSi ribbon specimen preannealed at 594K for 164 hours. The viscosity remained constant for several hours prior to specimen crystallization.

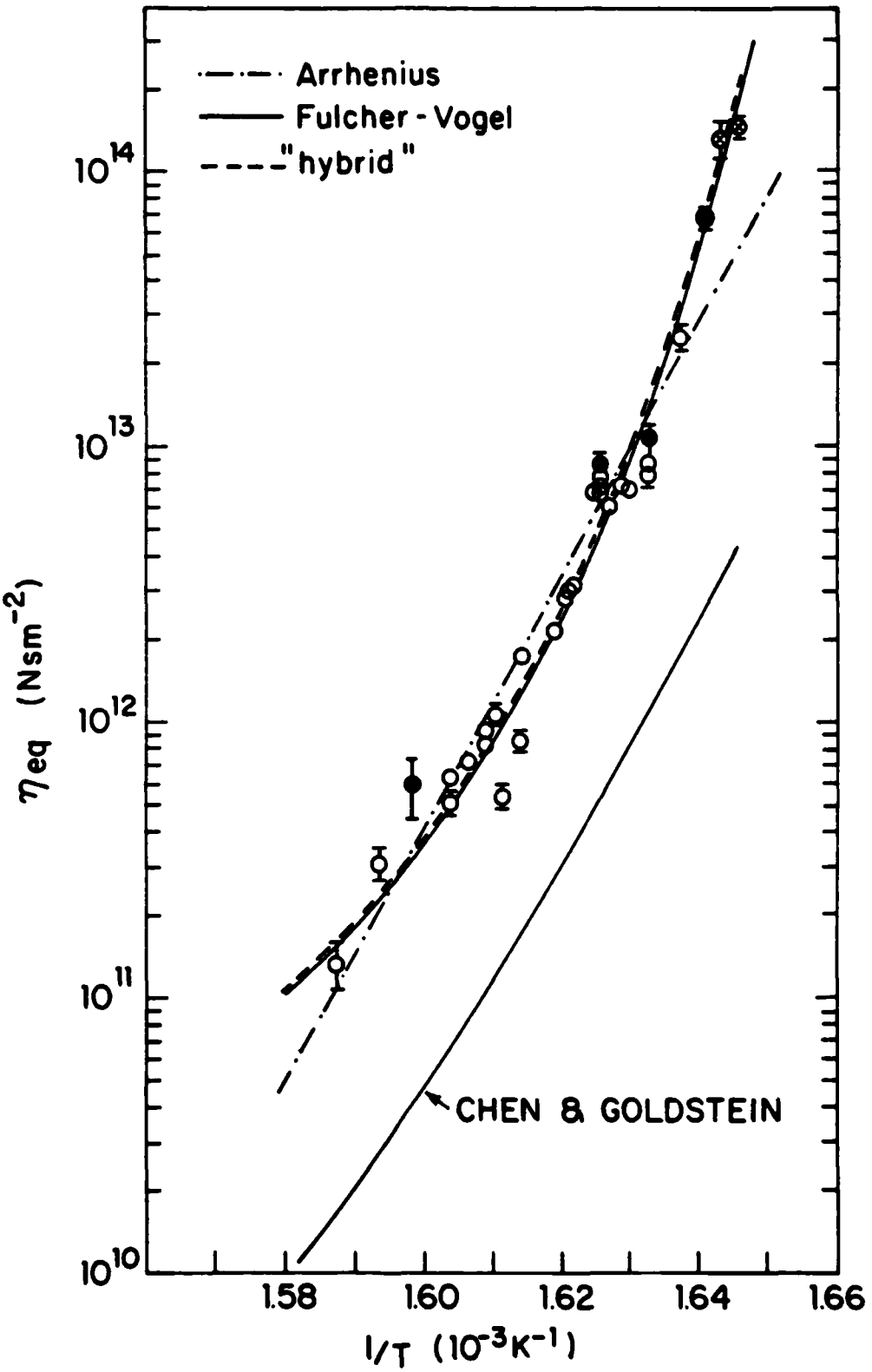


Figure 14

Summary of $\eta_{eq}$ values determined from model fits to increasing viscosity data (circles), decreasing viscosity data (dots), and direct measurements on specimens preannealed at low temperature (circled x). The temperature dependence of $\eta_{eq}$ is described well by the Fulcher-Vogel and "hybrid" equations. The Chen and Goldstein results are from ref. 8.

Table 1

MEASURED TIME FOR ANELASTIC DECAY AND ANELASTIC COMPLIANCE

| Run | Test Temperature (K) | Decay Time (min) | $\Delta\gamma_A/\Delta\tau$ ($10^{-11}m^2/N$) |
|---|---|---|---|
| A | 614 | 10 ± 1 | 9.0 ± 2.7 |
| B | 614 | 4.4 ± 1 | 6.3 ± 1.2 |
| C | 614 | 8.7 ± 2 | 10.0 ± 3.6 |
| D | 615 | 6.1 ± 1 | 7.9 ± 1.5 |
| E | 621 | 2.9 ± 1 | 8.7 ± 2.7 |

## REFERENCES


1. A.I. Taub and F. Spaepen, Acta Met. 28, 1781 (1980).
2. A.I. Taub and F. Spaepen, Scripta Met. 14, 1197 (1980).
3. A.I. Taub and F.E. Luborsky, Acta Met. 29, 1939 (1981).
4. J. Haimovich and T. Egami, Mater. Sci. Eng. 61, 89 (1983).
5. H.S. Chen and D. Turnbull, J. Chem. Phys. 48, 2560 (1968).
6. S.S. Tsao and F. Spaepen, in Amorphous Materials: Modeling of Structure and Properties, ed. by V. Vitek, New York: TMS-AIME, 1983.
7. A.I. Taub and F. Spaepen, Scripta Met. 13, 195 (1979).
8. H.S. Chen and M. Goldstein, J. Appl. Phys. 43, 174 (1971).
9. F. Spaepen, ''Physics of Defects'', in Les Houches Lectures XXXV, ed. by J.P. Poirier and M. Kleman, North Holland, 1981.
10. H.R. Lillie, J. Amer. Cer. Soc. 16, 619 (1933).
11. G.J. Roberts and J.P. Roberts, Proc. 7th Int. Conf. on Glass, 1965, p. 31.
12. P.R. Bevington, Data Reduction and Error Analysis for the Physical Sciences, New York: McGraw-Hill, 1961, p. 323.
13. A. Einstein, Ann. Phys. 19, 289 (1906).
14. J.W. Christian, The Theory of Transformations in Metals and Alloys, 2nd ed., London: Pergamon Press, 1975.
15. S.S. Tsao, Ph.D. Thesis, Harvard University (1983), Cambridge, Mass.
16. K.F. Kelton and F. Spaepen, to be published.
17. J.P. Patterson and D.R.H. Jones, Acta Met. 28, 675 (1980).
18. S.S. Tsao and F. Spaepen, Proc. 4th Int. Conf. on Rapidly Quenched Metals (Sendai, 1981), p. 463.
19. P.H. Gaskell, Glassy Metals II, Top. Appl. Phys. 53, ed. by H. Beck and H.J. Guntherodt, Berlin: Springer (1983), p. 5.

20. T. Egami, K. Maeda and V. Vitek, Phil. Mag. A 41, 883 (1980).

21. D.R. Nelson, Phys. Rev. B 28, 5515 (1983).

22. D.R. Nelson, Proc. Yamada Conf. IX on Dislocations in Solids, Tokyo, Aug. 26-31 (1984).

23. M. Cohen and D. Turnbull, J. Chem. Phys. 31, 1164 (1959).

24. G. Adam and J.H. Gibbs, J. Chem. Phys. 43, 139 (1965).

25. A. van den Beukel and S. Radelaar, Acta Met. 31, 419 (1983).

26. H.S. Chen, J. Appl. Phys. 49, 3289 (1978).

END

FILMED

12-84

DTIC